

Fast solution of fully implicit Runge-Kutta and discontinuous Galerkin in time for numerical PDEs, Part II: nonlinearities and DAEs*

Ben S. Southworth[†] Oliver A. Krzysik[‡] Will Pazner[§]

October 7, 2021

Abstract

Fully implicit Runge-Kutta (IRK) methods have many desirable accuracy and stability properties as time integration schemes, but high-order IRK methods are not commonly used in practice with large-scale numerical PDEs because of the difficulty of solving the stage equations. This paper introduces a theoretical and algorithmic framework for solving the nonlinear equations that arise from IRK methods (and discontinuous Galerkin discretizations in time) applied to nonlinear numerical PDEs, including PDEs with algebraic constraints. Several new linearizations of the nonlinear IRK equations are developed, offering faster and more robust convergence than the often-considered simplified Newton, as well as an effective preconditioner for the true Jacobian if exact Newton iterations are desired. Inverting these linearizations requires solving a set of block 2×2 systems. Under quite general assumptions, it is proven that the preconditioned 2×2 operator's condition number is bounded by a small constant close to one, *independent of the spatial discretization*, spatial mesh, and time step, and with only weak dependence on the number of stages or integration accuracy. Moreover, the new method is built using the same preconditioners needed for backward Euler-type time stepping schemes, so can be readily added to existing codes. The new methods are applied to several challenging fluid flow problems, including the compressible Euler and Navier Stokes equations, and the vorticity-streamfunction formulation of the incompressible Euler and Navier Stokes equations. Up to 10th-order accuracy is demonstrated using Gauss IRK, while in all cases 4th-order Gauss IRK requires roughly half the number of preconditioner applications as required by standard SDIRK methods.

1 Introduction

1.1 Fully implicit Runge-Kutta

Consider the method-of-lines approach to the numerical solution of partial differential equations (PDEs), where we discretize in space and arrive at a system of ordinary

*BSS was supported by Lawrence Livermore National Laboratory under contract B639443, and as a Nicholas C. Metropolis Fellow under the Laboratory Directed Research and Development program of Los Alamos National Laboratory. OAK acknowledges the support of an Australian Government Research Training Program (RTP) Scholarship.

[†]Theoretical Division, Los Alamos National Laboratory, U.S.A. (southworth@lanl.gov), <http://orcid.org/0000-0002-0283-4928>

[‡]School of Mathematics, Monash University, Australia (oliver.krzysik@monash.edu), <https://orcid.org/0000-0001-7880-6512>

[§]Center for Applied Scientific Computing, Lawrence Livermore National Laboratory, U.S.A. (pazner1@llnl.gov)

differential equations (ODEs) in time,

$$M\mathbf{u}'(t) = \mathcal{N}(\mathbf{u}, t) \quad \text{in } (0, T], \quad \mathbf{u}(0) = \mathbf{u}_0, \quad (1)$$

where M is a mass matrix and $\mathcal{N} : \mathbb{R}^N \times \mathbb{R}_+ \mapsto \mathbb{R}^N$ is a discrete, time-dependent, nonlinear operator depending on t and \mathbf{u} (including potential forcing terms). Note, PDEs with an algebraic constraint, for example, the divergence-free constraint in Navier Stokes, instead yield a system of differential algebraic equations (DAEs). DAEs require separate treatment and are addressed in [Section 6](#). Now, consider time propagation of (1) using an s -stage Runge-Kutta scheme, characterized by the Butcher tableaux $\frac{\mathbf{c}_0}{\mathbf{b}_0^T} \left| \begin{array}{c} A_0 \\ \mathbf{b}_0^T \end{array} \right.$, with Runge-Kutta matrix $A_0 = \{a_{ij}\} \in \mathbb{R}^{s \times s}$, weight vector $\mathbf{b}_0^T = (b_1, \dots, b_s)^T$, and abscissa $\mathbf{c}_0 = (c_1, \dots, c_s)$.

Runge-Kutta methods update the solution using a sum over stage vectors,

$$\mathbf{u}_{n+1} = \mathbf{u}_n + \delta t \sum_{i=1}^s b_i \mathbf{k}_i, \quad \text{where} \quad (2)$$

$$\mathbf{0} = M\mathbf{k}_i - \mathcal{N}\left(\mathbf{u}_n + \delta t \sum_{j=1}^s a_{ij} \mathbf{k}_j, t_n + \delta t c_i\right). \quad (3)$$

For nonlinear PDEs, \mathcal{N} is linearized using, for example, a Newton or a Picard linearization, and each nonlinear iteration then consists of solving the linearized system of equations. In most cases, such a linearization is designed to approximate (or equal) the Jacobian of (3). Applying the chain rule to (3) for the partial $\partial(M\mathbf{k}_i - \mathcal{N}_i)/\partial\mathbf{k}_j$, we see that the linearized system takes the form

$$\left(\begin{array}{ccc|ccc} M & & \mathbf{0} & a_{11}\mathcal{L}_1 & \dots & a_{1s}\mathcal{L}_1 \\ & \ddots & & \vdots & \ddots & \vdots \\ \mathbf{0} & & M & a_{s1}\mathcal{L}_s & \dots & a_{ss}\mathcal{L}_s \end{array} \right) - \delta t \begin{pmatrix} a_{11}\mathcal{L}_1 & \dots & a_{1s}\mathcal{L}_1 \\ \vdots & \ddots & \vdots \\ a_{s1}\mathcal{L}_s & \dots & a_{ss}\mathcal{L}_s \end{pmatrix} \begin{bmatrix} \mathbf{k}_1 \\ \vdots \\ \mathbf{k}_s \end{bmatrix} = \begin{bmatrix} \mathbf{f}_1 \\ \vdots \\ \mathbf{f}_s \end{bmatrix}, \quad (4)$$

where $\mathcal{L}_i \in \mathbb{R}^{N \times N}$ denotes a linearization of the nonlinear function corresponding to the i th stage vector, $\mathcal{N}_i := \mathcal{N}\left(\mathbf{u}_n + \delta t \sum_{j=1}^s a_{ij} \mathbf{k}_j, t_n + \delta t c_i\right)$, and $-\mathbf{f}_i$ corresponds to (3) evaluated at the previous nonlinear iterate for $\{\mathbf{k}_i\}$ (i.e., \mathbf{f}_i is the negative residual of (3) from the previous iterate). We emphasize that the spatially linearized operators, \mathcal{L}_i , should be fixed for a given block row of the full linearized system, as in (4). Moving forward, we let \mathcal{L} refer to a general, spatially linearized operator when the stage index is not relevant.

The difficulty in fully implicit Runge-Kutta methods (which we will denote IRK) lies in solving the $Ns \times Ns$ block linear system in (4). This paper focuses on the parallel simulation of numerical PDEs, where N is typically very large and \mathcal{L} is highly ill-conditioned. In such cases, direct solution techniques to solve (4) are not a viable option, and fast, parallel iterative methods must be used. However, IRK methods are rarely employed in practice due to the difficulties of solving (4). Even for relatively simple parabolic PDEs where $-\mathcal{L}$ is symmetric positive definite (SPD), (4) is a large nonsymmetric matrix with significant block coupling. For nonsymmetric matrices \mathcal{L} that already have inter-variable coupling that arise in systems of PDEs, traditional iterative methods are even less likely to yield acceptable performance in solving (4).

Remark 1 (Discontinuous Galerkin (DG) in time). *For completeness, here we repeat the discussion from the companion paper [46] regarding the relation of DG discretizations in time to IRK methods. After linearization, DG discretizations in time give rise to linear*

algebraic systems of the form

$$\left(\begin{bmatrix} \delta_{11}M & & \delta_{1s}M \\ & \ddots & \\ \delta_{s1}M & & \delta_{ss}M \end{bmatrix} - \delta t \begin{bmatrix} t_{11}\mathcal{L}_1 & \dots & t_{1s}\mathcal{L}_1 \\ \vdots & \ddots & \vdots \\ t_{s1}\mathcal{L}_s & \dots & t_{ss}\mathcal{L}_s \end{bmatrix} \right) \begin{bmatrix} \mathbf{u}_1 \\ \vdots \\ \mathbf{u}_s \end{bmatrix} = \begin{bmatrix} \mathbf{r}_1 \\ \vdots \\ \mathbf{r}_s \end{bmatrix}. \quad (5)$$

The coefficients t_{ij} correspond to a temporal mass matrix, the coefficients δ_{ij} correspond to a DG weak derivative with upwind numerical flux, and the unknowns \mathbf{u}_i are the coefficients of the polynomial expansion of the approximate solution (for example, see [1, 25, 29, 43]). Both of the coefficient matrices $\{t_{ij}\}, \{\delta_{ij}\}$ are invertible. It can be seen that the algebraic form of the DG in time discretization is closely related to the implicit Runge-Kutta system (4) and, in fact, (5) can be recast in the form of (4) using the invertibility of the matrix $\{\delta_{ij}\}$. In particular, the degree- p DG method using $(p+1)$ -point Radau quadrature, which is exact for polynomials of degree $2p$, is equivalent to the Radau IIA collocation method [29], which is used for many of the numerical results in Section 7. Thus, although the remainder of this paper focuses on fully implicit Runge-Kutta, the algorithms developed here can also be applied to DG discretizations in time on fixed slab-based meshes.

1.2 Outline

In [46], robust and effective preconditioning techniques are developed for the solution of fully implicit Runge Kutta methods and DG discretizations in time applied to linear numerical PDEs. This paper builds on ideas from [46] to address nonlinearities and DAEs.

First, new ways to approximate (4) are introduced in Section 3, which can be used as preconditioners for solving (4) exactly, or as a modified linearization. The new approach only requires the solution of a block 2×2 set of equations for each pair of stages, rather than the fully coupled $s \times s$ system in (4). Moreover, unlike many of the simplified Newton approaches seen previously in the literature, the new approach can yield convergence comparable to true Newton iterations (or be used as a very effective preconditioner of the true Jacobian).

Section 4 then introduces block preconditioners for the 2×2 systems, where the preconditioned Schur-complement (which effectively defines convergence of fixed-point and Krylov iterations applied to the larger 2×2 system [47]) is proven to have a condition number bounded by a small order-one constant. The preconditioner is *asymptotically optimal*, that is, the condition number is bounded independent of mesh spacing and time step, and has only weak dependence on the order of integration/number of stages. The theory is quite general, relying on only basic stability assumptions from Section 2.2, and the block preconditioning only requires an effective preconditioner for systems along the lines of $\gamma M - \delta t \mathcal{L}$, exactly as would be used, e.g., for SDIRK methods. A self-contained algorithm description is provided in Section 5.

Numerical results for several challenging nonlinear fluid flow problems are provided in Section 7. These include the compressible Euler equations, for which we solve a model isentropic vortex problem, and the compressible Navier–Stokes equations, for which we consider wall-resolved high Reynolds number flow over a NACA airfoil. Additionally, we consider two test cases using the incompressible Euler and Navier–Stokes equations in vorticity-streamfunction formulation. After spatial discretization, these equations result in a system of index-1 differential algebraic equations (DAEs), illustrating the applicability of the IRK linearizations and preconditioners to systems of equations with algebraic constraints.

The methods are implemented with the MFEM [2] library and available at <https://github.com/bensworth/IRKIntegration>.

2 Background

2.1 Why fully implicit and previous work

Aside from the difficulty of solving (4) rapidly for large, ill-conditioned $\{\mathcal{L}_i\}$, IRK methods have a number of desirable properties in practice. For stiff PDEs, the observed accuracy of Runge-Kutta methods can be limited to $\approx \min\{p, q + 1\}$, for integration order p and stage-order q [15, 24]. For index-2 DAEs, the order of accuracy is formally limited to that of the stage order, q [15]. Diagonally implicit Runge Kutta (DIRK) methods are most commonly used in practice for numerical PDEs due to ease of implementation, but DIRK methods have a maximum order of $p = s$ or $p = s + 1$ with reasonable stability properties [15, Section IV.6],[24] and, moreover, are limited to stage-order $q = 1$ [41] (or $q = 2$ for ESDIRK methods with one explicit stage [24]). In contrast, IRK methods can have order as high as $p = 2s$ for s stages and stage-order $q = s$. Advantages of IRK methods (in a discretization sense) for the system of DAEs that arise in incompressible Navier Stokes can be seen in [42], where high-order accuracy can be obtained in the pressure variable without additional projections, splittings, or staggered grids. For PDEs where DIRK methods are ineffective, linear multistep methods, in particular BDF schemes, can offer improved accuracy and are often used in practice. However, A-stable implicit multistep methods can have at most order two, and the stability region of higher-order methods moves progressively farther away from the imaginary axis, which is particularly problematic for advection-dominated flows. Multistep methods also introduce their own difficulties in initializing (or restarting after discontinuities) with high-order accuracy, due to their multistep nature [7, Chapter 4], whereas Runge-Kutta methods naturally start with high-order accuracy. Furthermore, neither linear multistep nor explicit Runge Kutta methods can be generally symplectic (i.e., for non-separable problems) [17]. Although DIRK methods can be symplectic, they are limited to at most 4th order and, moreover, known methods above second order are impractical due to negative diagonal entries of A_0 (leading to a negative shift rather than positive shift of the spatial discretization) [24]. IRK methods are able to satisfy conditions for symplecticity of arbitrary order, and even moderate-order symplectic integration requires IRK methods.

It should be noted that IRK methods are by no means new, and many papers have considered the efficient implementation of IRK integration in various contexts. Much of the early work was focused on ODEs and minimizing the number of LU decompositions that must be computed. Most of these works use a simplified Newton method, where it is assumed that $\mathcal{L}_i = \mathcal{L}_j$ for all i, j , and either consider the solution of the simplified system (4) (see, e.g., [6, 8, 19, 21, 50]), or introduce/analyze a modified nonlinear iteration or time stepping scheme (see, e.g., [10, 11, 13, 14, 18, 20]). Some of the first works to consider IRK methods for PDEs were the sequence of papers [32, 33, 48], which analyze block triangular and diagonal preconditioners for the (linear) diffusion and bi-domain equations in the Sobolev setting, and demonstrate that the preconditioned operators are well-conditioned. Other papers have demonstrated success with various IRK preconditioning strategies for parabolic type problems as well [4, 9, 26, 39, 45], with the method in [4] also demonstrating success in practice on linear hyperbolic problems. Nevertheless, very few works have considered the true nonlinear setting for numerical PDEs (that is, not simplified Newton) and, to our knowledge, no works have provided analysis of preconditioning (4) for non-parabolic problems. This work addresses both of these issues.

Remark 2 (Growing interest in IRK). *While writing this paper, at least three preprints have been posted studying the use of IRK methods for numerical PDEs. Two papers develop new block preconditioning techniques for parabolic PDEs [22, 37] ([22] also ap-*

peals to the Schur decomposition as used in this paper), and one focuses on a numerical implementation of IRK methods with the Firedrake package [12].

2.2 A preconditioning framework and stability

Similar to [34, 46], methods developed in this paper appeal to pulling $(A_0 \otimes I)$ out of the matrix in (4), yielding an equivalent problem

$$\left(A_0^{-1} \otimes M - \delta t \begin{bmatrix} \mathcal{L}_1 & & \\ & \ddots & \\ & & \mathcal{L}_s \end{bmatrix} \right) (A_0 \otimes I) \begin{bmatrix} \mathbf{k}_1 \\ \vdots \\ \mathbf{k}_s \end{bmatrix} = \begin{bmatrix} \mathbf{f}_1 \\ \vdots \\ \mathbf{f}_s \end{bmatrix}. \quad (6)$$

Off-diagonal blocks in the reformulated system (6) now consist of mass matrices, rather than differential operators, which simplifies the development and analysis of preconditioning, and also reduces the number of sparse matrix-vector operations with $\{\mathcal{L}_i\}$. Algorithms developed in this paper rely on the following assumption regarding eigenvalues of A_0 and A_0^{-1} :

Assumption 1. *Assume that all eigenvalues of A_0 (and equivalently A_0^{-1}) have positive real part.*

Recall that if an IRK method is A-stable, irreducible, and A_0 is invertible (which includes DIRK, Gauss, Radau IIA, and Lobatto IIIC methods, among others), then Assumption 1 holds [15]; that is, Assumption 1 is straightforward to satisfy in practice.

The second assumption we make for analysis in this paper is derived from stability of ODE solvers applied to numerical PDEs using the method-of-lines. The Dahlquist test problem extends naturally to this setting, where we are interested in the stability of the linearized operator \mathcal{L} , for the ODE(s) $\mathbf{u}'(t) = \mathcal{L}\mathbf{u}$, with solution $e^{t\mathcal{L}}\mathbf{u}$. In [38], necessary and sufficient conditions for stability are derived as the ε pseudo-eigenvalues of $\delta t\mathcal{L}$ being within $\mathcal{O}(\varepsilon) + \mathcal{O}(\delta t)$ of the stability region as $\varepsilon, \delta t \rightarrow 0$. Here we relax this assumption to something that is more tractable to work with by noting that the ε pseudo-eigenvalues are contained within the field of values to $\mathcal{O}(\varepsilon)$ [49, Eq. (17.9)], where the field of values is defined as

$$W(\mathcal{L}) := \{ \langle \mathcal{L}\mathbf{x}, \mathbf{x} \rangle : \|\mathbf{x}\| = 1 \}. \quad (7)$$

This motivates the following assumption for the analysis done in this paper:

Assumption 2. *Let \mathcal{L} be a linearized spatial operator, and assume that $W(\mathcal{L}) \leq 0$ (that is, $W(\mathcal{L})$ is a subset of the closed left half plane).*

Note that if \mathcal{L} is normal, then Assumption 2 is equivalent to the real parts of the eigenvalues of \mathcal{L} being in the closed left-half plane since $W(\mathcal{L})$ is the convex hull of the eigenvalues.

As discussed in [46], note that the field of values has an additional connection to stability. From [49, Theorem 17.1], we have that $\|e^{t\mathcal{L}}\| \leq 1$ for all $t \geq 0$ if and only if $W(\mathcal{L}) \leq 0$. This is analogous to the “strong stability” discussed by Leveque [27, Chapter 9.5], as opposed to the weaker (but still sufficient) condition $\|e^{t\mathcal{L}}\| \leq C$ for all $t \geq 0$ and some constant C . In practice, Assumption 2 often holds when simulating numerical PDEs, and in Section 4 it is proven that Assumption 1 and 2 guarantee the preconditioning methods proposed here yield a preconditioned Schur complement with a small, bounded, order-one condition number, within the larger 2×2 systems discussed in Section 1.2.

3 Nonlinear iterations

Let $\lambda_{\pm} := \eta \pm i\beta$ denote an eigenvalue (pair) of A_0^{-1} , where, under [Assumption 1](#), $\eta > 0$. For ease of notation, in this section and [Section 4](#), we will scale both sides of (6) by a block diagonal operator, with diagonal blocks M^{-1} , and define $\widehat{\mathcal{L}}_i := \delta t M^{-1} \mathcal{L}_i$, for $i = 1, \dots, s$. In practice we do *not* directly form $\widehat{\mathcal{L}}$, as M^{-1} is often a dense matrix. Rather, it is a theoretical tool to simplify notation; in practice we must apply and precondition standard time-dependent operators of the form $(\gamma M - \delta t \mathcal{L}_i)$.

3.1 Simplified Newton

Suppose $\mathcal{L}_i = \mathcal{L}_j$ for all i, j (as in a simplified Newton method). Then, the linear system for stage vectors (6) (diagonally scaled by M^{-1}) can be written in condensed Kronecker product notation

$$\left(A_0^{-1} \otimes I - I \otimes \widehat{\mathcal{L}} \right) (A_0 \otimes I) \mathbf{k} = (I_s \otimes M^{-1}) \mathbf{f}. \quad (8)$$

Now, let $A_0^{-1} = Q_0 R_0 Q_0^T$ be the real Schur decomposition of A_0^{-1} , where Q_0 is real-valued and orthogonal, and R_0 is a block upper triangular matrix, where each block corresponds to an eigenvalue (pair) of A_0^{-1} . Real-valued eigenvalues have block size one, and complex eigenvalues $\eta \pm i\beta$ are in 2×2 blocks, $\begin{bmatrix} \eta & \phi \\ -\beta^2/\phi & \eta \end{bmatrix}$, for some constant ϕ . Pulling out a $Q_0 \otimes I$ and $Q_0^T \otimes I$ from the left and right of (8) yields the equivalent linear system

$$\left(R_0 \otimes I - I \otimes \widehat{\mathcal{L}} \right) (R_0^{-1} Q_0^T \otimes I) \mathbf{k} = (Q_0^T \otimes I) (I_s \otimes M^{-1}) \mathbf{f}. \quad (9)$$

The left-most matrix is now block upper triangular, which can be solved using block backward substitution, and requires inverting each diagonal block. Diagonal blocks corresponding to real-valued eigenvalues η take the form $(\eta I - \widehat{\mathcal{L}})$, and are amenable to standard preconditioning techniques as used, e.g., for backward Euler. While 2×2 diagonal blocks corresponding to complex eigenvalues take the form $\begin{bmatrix} \eta I - \widehat{\mathcal{L}} & \phi I \\ -\frac{\beta^2}{\phi} I & \eta I - \widehat{\mathcal{L}} \end{bmatrix}$. Effective block preconditioners for such matrices are developed in [Section 4](#), including theory guaranteeing the (inner) preconditioned Schur complement has a small, bounded, order-one condition number.

Remark 3 (Real Schur decomposition). *A real Schur decomposition is not new to Runge-Kutta literature and is most notably used in the RADAU code [16]. The key contribution here for the simplified Newton setting is proving a robust and general way to precondition the resulting operators in the context of numerical PDEs (see [Section 4](#)). Moreover, the real Schur decomposition applied to the simplified Newton setting after pulling out an $A_0^{-1} \otimes I$ provides the key motivation for the development of more general nonlinear iterations introduced in the following section.*

3.2 General nonlinear iterations

Note that most nonlinear iterations, including Newton, Picard, and other fixed-point iterations, can all be expressed as linearly preconditioned nonlinear Richardson iterations. For nonlinear functional $\mathcal{F}(\mathbf{x}) = 0$, such an iteration takes the form

$$\mathbf{x}_{k+1} = \mathbf{x}_k + \mathcal{P}^{-1} \mathcal{F}(\mathbf{x}_k). \quad (10)$$

For preconditioner $\mathcal{P} := -J[\mathbf{x}_k]$ given by the (negative) Jacobian of $\mathcal{F}(\mathbf{x})$ evaluated at \mathbf{x}_k , (10) yields a Newton iteration. For \mathcal{P} given by a zero-th order linearization of $\mathcal{F}(\mathbf{x})$ (the nonlinear operator evaluated at \mathbf{x}_k), (10) yields a Picard iteration. In general, thinking of nonlinear iterations as linear preconditioners for nonlinear Richardson iterations (10) naturally allows for various levels of approximation, which is the focus of this section.

Now let us return to (6) for $\mathcal{L}_i \neq \mathcal{L}_j$, but extract the real Schur decomposition as in Section 3.2. Continuing with the simplified representation $\widehat{\mathcal{L}}_i := \delta t M^{-1} \mathcal{L}_i$, this yields the linear system

$$\left(R_0 \otimes I - (Q_0^T \otimes I) \begin{bmatrix} \widehat{\mathcal{L}}_1 & & \\ & \ddots & \\ & & \widehat{\mathcal{L}}_s \end{bmatrix} (Q_0 \otimes I) \right) (R_0^{-1} Q_0^T \otimes I) \mathbf{k} = (Q_0^T \otimes I) \mathbf{f}. \quad (11)$$

Picard and Newton iterations both require the solution of such a system each iteration (see \mathcal{P}^{-1} in (10)). Here we propose approximations to the solution of (11) that are (i) solvable using techniques similar to the simplified Newton setting in Section 3.1, and (ii) yield nonlinear convergence close to a true Newton or Picard iteration. In principle, these approximations can also be iterated to convergence in the linear sense, yielding a precise Newton or Picard iteration, but here we opt to apply the approximation directly as the nonlinear preconditioner, resolving the error between the approximation and an exact Newton/Picard iteration in the outer nonlinear iteration. Similar to inexact Newton methods, such approaches are often more efficient in practice than the corresponding exact methods.

To develop effective approximations, we are particularly interested in the operator

$$\widehat{P} := (Q_0^T \otimes I) \begin{bmatrix} \widehat{\mathcal{L}}_1 & & \\ & \ddots & \\ & & \widehat{\mathcal{L}}_s \end{bmatrix} (Q_0 \otimes I) = \begin{bmatrix} \mathbf{d}_{1,1}^T \widehat{\mathcal{L}} & \cdots & \mathbf{d}_{1,s}^T \widehat{\mathcal{L}} \\ \vdots & & \vdots \\ \mathbf{d}_{s,1}^T \widehat{\mathcal{L}} & \cdots & \mathbf{d}_{s,s}^T \widehat{\mathcal{L}} \end{bmatrix}, \quad (12)$$

where $\mathbf{d}_{k,\ell}^T = \left((Q_0^T)_{k,1} (Q_0)_{1,\ell}, \dots, (Q_0^T)_{k,s} (Q_0)_{s,\ell} \right) \in \mathbb{R}^s$ is a scalar row vector, $\widehat{\mathcal{L}} = (\widehat{\mathcal{L}}_1; \dots; \widehat{\mathcal{L}}_s)$ is a block column vector of the linearized operators, and

$$\mathbf{d}_{k,\ell}^T \widehat{\mathcal{L}} = \sum_{i=1}^s (d_{k,\ell})_i \widehat{\mathcal{L}}_i.$$

Note that the vector $\mathbf{d}_{k,\ell}$ represents the element-wise product between the k th row of Q_0^T and the ℓ th column of Q_0 . By the orthogonality of Q_0 , we have $\sum_{i=1}^s (d_{k,\ell})_i = \delta_{k,\ell}$, where $\delta_{k,\ell}$ is the Kronecker delta. Thus, when $\widehat{\mathcal{L}}_i = \widehat{\mathcal{L}}_j$, (12) is block diagonal, given by $I \otimes \widehat{\mathcal{L}}$. Due to the off-diagonal zero sums, here we claim that (12) can be well-approximated by some block-diagonal matrix or block upper triangular matrix. Adding $R_0 \otimes I$ to such an approximation then yields an approximation to (11), which can be easily inverted using block backward substitution.

As an example, consider the matrix \widehat{P} from (12) for the two-stage Gauss and Radau IIA methods in bracket notation (to three digits of accuracy) where $\{a_1, a_2\} \mapsto a_1 \widehat{\mathcal{L}}_1 + a_2 \widehat{\mathcal{L}}_2$:

$$\text{Gauss(4): } \begin{bmatrix} \{1, 0\} & \{0, 0\} \\ \{0, 0\} & \{0, 1\} \end{bmatrix}, \quad \text{Radau IIA(3): } \begin{bmatrix} \{0.985, 0.015\} & \{0.121, -0.121\} \\ \{0.121, -0.121\} & \{0.015, 0.985\} \end{bmatrix}. \quad (13)$$

Note that there is no approximation in two-stage Gauss because the operator (12) is already block diagonal, that is, it is straightforward to apply a true Newton or Picard iteration to two-stage Gauss using analogous block-preconditioning techniques as used for simplified Newton. For two-stage Radau IIA, we see that the diagonal blocks are almost defined by the (linearized) operator evaluated at a single time step, which provides a natural and simple approximation. The off-diagonal blocks are simply the difference between successive stages, $0.121(\widehat{\mathcal{L}}_1 - \widehat{\mathcal{L}}_2)$. Such entries could be included in the preconditioning for the upper triangular portion of the matrix (adding a few additional matrix-vector products and some memory usage), or simply ignored altogether under the assumption that $0.121(\widehat{\mathcal{L}}_1 - \widehat{\mathcal{L}}_2)$ is “small” relative to the diagonal blocks in some sense. Even for reasonably stiff problems, the operator often does not change substantially between two stages. Large changes in the operator between temporal stages are often an indication that the time step is too large to adequately resolve the nonlinear behavior of the equations. Similar structure as discussed for the two-stage methods holds for other methods as well.

Motivated by the above discussion, we consider Newton-like methods (or more generally some fixed-point iteration as in (10)) which use approximate Jacobians having a (block) sparsity pattern contained within that of $R_0 \otimes I$. That is, we replace the \widehat{P} operator (12) in the true Jacobian (11) with a block upper triangular approximation $\widetilde{P} \approx \widehat{P}$. Recall by constructing \widetilde{P} to be block upper triangular, we can then invert the resulting operator $R_0 \otimes I - \widetilde{P}$ via block backward substitution, preconditioning each 1×1 or 2×2 diagonal block similar to the simplified Newton setting in Section 3.1 (formal details on preconditioning are introduced in Section 4). In addition to the simplified Newton method discussed in Section 3.1, we propose the following three (successively more accurate) approximations to (12). As an example, for each of the following approximations, the matrix \widetilde{P} derived from \widehat{P} in (13) for the 2-stage Radau IIA(3) scheme is also shown.

0. Simplified Newton: As in Section 3.1, apply a simplified Newton method by evaluating \mathcal{L} at the same time point for all stages. That is, $\widetilde{P} = I \otimes \widehat{\mathcal{L}}_k$ for some k .

$$\text{Radau IIA(3): } \widetilde{P} = \begin{bmatrix} \widehat{\mathcal{L}}_k & 0 \\ 0 & \widehat{\mathcal{L}}_k \end{bmatrix}.$$

1. Newton-like(1): Truncate \widehat{P} (12) to be block diagonal and lump the coefficients of each diagonal term $\mathbf{d}_{i,i}$ to the largest one so that each diagonal block of \widetilde{P} contains only one matrix from $\widehat{\mathcal{L}}$. That is, the i th diagonal block of \widetilde{P} is $\widehat{\mathcal{L}}_k$, where $k = \arg \max (|(d_{i,i})_1|, \dots, |(d_{i,i})_s|)$.

$$\text{Radau IIA(3): } \widetilde{P} = \begin{bmatrix} \widehat{\mathcal{L}}_1 & 0 \\ 0 & \widehat{\mathcal{L}}_2 \end{bmatrix}.$$

2. Newton-like(2): Truncate \widehat{P} (12) to be block diagonal. That is, the i th diagonal block of \widetilde{P} is $\mathbf{d}_{i,i}^T \widehat{\mathcal{L}}$.

$$\text{Radau IIA(3): } \widetilde{P} = \begin{bmatrix} 0.985\widehat{\mathcal{L}}_1 + 0.015\widehat{\mathcal{L}}_2 & 0 \\ 0 & 0.015\widehat{\mathcal{L}}_1 + 0.985\widehat{\mathcal{L}}_2 \end{bmatrix}.$$

3. Newton-like(3): Truncate \widehat{P} (12) inside the block upper triangular sparsity pattern of $R_0 \otimes I$. This option adds a number of matrix-vector products, but is also the

best approximation to an exact Newton or Picard iteration (and corresponds to an exact Newton iteration for 2-stage methods).

$$\text{Radau IIA(3): } \tilde{P} = \begin{bmatrix} 0.985\hat{\mathcal{L}}_1 + 0.015\hat{\mathcal{L}}_2 & 0.121\hat{\mathcal{L}}_1 - 0.121\hat{\mathcal{L}}_2 \\ 0.121\hat{\mathcal{L}}_1 - 0.121\hat{\mathcal{L}}_2 & 0.015\hat{\mathcal{L}}_1 + 0.985\hat{\mathcal{L}}_2 \end{bmatrix}.$$

Of course there are other combinations possible, including using, e.g., Newton-like(1) as a preconditioner for Newton-like(3), but we do not elaborate for the sake of space.

4 Linear preconditioning theory

The methods derived in [Section 3](#) use block backward substitution which requires solving 2×2 block systems along the lines of

$$\begin{bmatrix} \eta I - \mathbf{d}_{1,1}^T \hat{\mathcal{L}} & \phi I - \mathbf{d}_{1,2}^T \hat{\mathcal{L}} \\ -\frac{\beta^2}{\phi} I - \mathbf{d}_{2,1}^T \hat{\mathcal{L}} & \eta I - \mathbf{d}_{2,2}^T \hat{\mathcal{L}} \end{bmatrix}, \quad (14)$$

with the off-diagonal blocks only including non-identity terms for method 3 from [Section 3.2](#). As discussed previously, we expect the non-identity off-diagonal terms to typically be small. This section consider block preconditioning of the general linear problem that arises in methods (0), (1), and (2), or methods (3) by neglecting non-identity off-diagonal coupling in (14) arising from the $\mathbf{d}_{1,2}^T \hat{\mathcal{L}}$ and $\mathbf{d}_{2,1}^T \hat{\mathcal{L}}$ terms:

$$\begin{bmatrix} \eta I - \hat{\mathcal{L}}_1 & \phi I \\ -\frac{\beta^2}{\phi} I & \eta I - \hat{\mathcal{L}}_2 \end{bmatrix}, \quad (15)$$

for some $\eta > 0, \phi \neq 0$. Note, excusing the slight abuse of notation, for ease of notation we have let $\hat{\mathcal{L}}_i = \mathbf{d}_{i,i}^T \hat{\mathcal{L}}$ denote the approximate operator from linearization method (0), (1), and (2), or (3), rather the direct linearization about the k th stage vector as used elsewhere in this paper. In practice the block preconditioning methods developed in this section have proven equally robust on systems resulting from nonlinear method (3) as those resulting from methods (1) and (2) (for which the theory applies), indicating that (15) is a suitable proxy for (14) for theoretical purposes. In (15) it is assumed that $W(\hat{\mathcal{L}}_i) \leq 0$ for $i = 1, 2$ ([Assumption 2](#)).¹ We will solve (15) using Krylov methods with block lower-triangular preconditioners of the form

$$L_P := \begin{bmatrix} \eta I - \hat{\mathcal{L}}_1 & \mathbf{0} \\ -\frac{\beta^2}{\phi} I & \hat{S} \end{bmatrix}^{-1}, \quad (16)$$

where \hat{S} is some approximation to the Schur complement of (15), which is given by

$$S := \eta I - \hat{\mathcal{L}}_2 + \beta^2(\eta I - \hat{\mathcal{L}}_1)^{-1}. \quad (17)$$

When applying GMRES to block 2×2 operators preconditioned with a lower (or upper) triangular preconditioner as in (16), convergence is exactly defined by convergence of GMRES applied to the preconditioned Schur complement, $\hat{S}^{-1}S$ [47]. If $\hat{S} = S$ is exact, exact convergence on the larger 2×2 system is guaranteed in two iterations (or one iteration with block LDU). This section focuses on the development of robust

¹Note that for nonlinear method (2), we are taking a weighted sum of operators that satisfy [Assumption 2](#). Due to the non-negativity of the weights, the summation also satisfies [Assumption 2](#).

preconditioners for the Schur complement (17). In particular, we develop a preconditioner for S such that the preconditioned operator has a bounded condition number, independent of $\widehat{\mathcal{L}}_1$ and $\widehat{\mathcal{L}}_2$, and with only weak dependence on the order of time integration. The preconditioner is also *asymptotically optimal* in the sense that the condition number is bounded independent of mesh spacing and time step. The analysis derived herein is based on the assumption that a small, bounded condition number corresponds to better preconditioners for nonsymmetric matrices.

As a result of [Assumption 2](#), the second term in (17), $(\eta I - \widehat{\mathcal{L}}_1)^{-1}$ is a compact operator adding a small positive perturbation to $\eta I - \widehat{\mathcal{L}}_2$. To that end, we approximate it with an identity perturbation and consider preconditioners of the form

$$\widehat{S}_\gamma := \gamma I - \widehat{\mathcal{L}}_2 \quad (18)$$

for some $\gamma > 0$. [Section 4.1](#) considers the simpler case of $\widehat{\mathcal{L}}_1 = \widehat{\mathcal{L}}_2$, deriving tight bounds on the conditioning of the preconditioned operator as well as an optimal choice of $\gamma \mapsto \gamma_*$ that minimizes the maximum condition number taken over all $\widehat{\mathcal{L}}$. [Section 4.2](#) then extends the theory to the more general $\widehat{\mathcal{L}}_1 \neq \widehat{\mathcal{L}}_2$. Under an additional assumption that $\widehat{\mathcal{L}}_1$ and $\widehat{\mathcal{L}}_2$ are “close” in some sense, the condition number of the preconditioned operator is bounded via $\text{cond}(\widehat{S}_{\gamma_*}^{-1} S) \leq 2 + \frac{\beta^2}{\eta^2}$, which is only a factor of two larger than the tight bounds derived for $\widehat{\mathcal{L}}_1 = \widehat{\mathcal{L}}_2$.

In practice, we typically do not want to apply $(\eta I - \widehat{\mathcal{L}}_1)^{-1}$ or \widehat{S}_γ^{-1} exactly for each iteration of the preconditioner (16). It is well-known in the block-preconditioning community that a few iterations of an effective preconditioner, such as multigrid, to represent the inverse of diagonal blocks in (16) typically yields convergence on the larger 2×2 operator just as fast as if performing direct solves, at a fraction of the cost. Thus, in practice we propose a block-triangular preconditioner similar to (16), but which only applies some approximation to the diagonal block inverses, $(\eta I - \widehat{\mathcal{L}}_1)^{-1}$ and $\widehat{S}^{-1} := (\gamma_* I - \widehat{\mathcal{L}}_2)^{-1}$ for a specific γ_* introduced in the following section.

4.1 $\widehat{\mathcal{L}}_1 = \widehat{\mathcal{L}}_2$

Consider right preconditioning the Schur complement with preconditioner $(\gamma I - \widehat{\mathcal{L}}_2)^{-1}$. The preconditioned Schur complement takes the form

$$\begin{aligned} \mathcal{P}_\gamma &:= \left[\eta I - \widehat{\mathcal{L}}_2 + \beta^2 (\eta I - \widehat{\mathcal{L}}_1)^{-1} \right] (\gamma I - \widehat{\mathcal{L}}_2)^{-1} \\ &= \left[(\eta^2 + \beta^2) I - \eta (\widehat{\mathcal{L}}_1 + \widehat{\mathcal{L}}_2) + \widehat{\mathcal{L}}_2 \widehat{\mathcal{L}}_1 \right] (\eta I - \widehat{\mathcal{L}}_1)^{-1} (\gamma I - \widehat{\mathcal{L}}_2)^{-1}. \end{aligned} \quad (19)$$

Making the simplification $\widehat{\mathcal{L}}_1 = \widehat{\mathcal{L}}_2 = \widehat{\mathcal{L}}$, \mathcal{P}_γ takes the simplified form

$$\mathcal{P}_\gamma = \left[(\eta^2 + \beta^2) I - 2\eta \widehat{\mathcal{L}} + \widehat{\mathcal{L}}^2 \right] (\eta I - \widehat{\mathcal{L}})^{-1} (\gamma I - \widehat{\mathcal{L}})^{-1}. \quad (20)$$

The following theorem (restated from [46, Th. 5]) tightly bounds the condition number of a slightly more general operator than the preconditioned Schur complement (20), and proves the optimality of a certain $\gamma_* \in (0, \infty)$ in term of minimizing the maximum condition number over all $\widehat{\mathcal{L}}$. The corollary following it provides tight bounds on the condition number of (20) for the optimal choice of $\gamma = \gamma_*$. Although the resulting conditioning here is slightly worse than can be achieved with the method designed specifically for linear PDEs [46, Cor. 6], [Table 1](#) shows that for up to 10th-order integration, at worst the preconditioned Schur complement has condition number on the order of 2–3.

Theorem 1 (Tight bounds on condition number, $\widehat{\mathcal{L}}_1 = \widehat{\mathcal{L}}_2$ [46]). Let $\widehat{\mathcal{L}}$ be real valued and suppose *Assumptions 1* and *2* hold, that is, $\eta > 0$ and $W(\widehat{\mathcal{L}}) \leq 0$. Let $\mathcal{P}_{\delta,\gamma}$ denote the preconditioned operator

$$\mathcal{P}_{\delta,\gamma} := [(\eta I - \widehat{\mathcal{L}})^2 + \beta^2 I](\delta I - \widehat{\mathcal{L}})^{-1}(\gamma I - \widehat{\mathcal{L}})^{-1}, \quad \delta, \gamma \in (0, \infty), \quad (21)$$

in which $[(\eta I - \widehat{\mathcal{L}})^2 + \beta^2 I]$ is preconditioned with $(\delta I - \widehat{\mathcal{L}})^{-1}(\gamma I - \widehat{\mathcal{L}})^{-1}$, for $\delta, \gamma \in (0, \infty)$. Let $\kappa(\mathcal{P}_{\delta,\gamma})$ denote the two-norm condition number of $\mathcal{P}_{\delta,\gamma}$, and define γ_* by $\gamma_* := \frac{\eta^2 + \beta^2}{\delta}$. Then

$$\kappa(\mathcal{P}_{\delta,\gamma_*}) \leq \frac{1}{2\eta} \left(\delta + \frac{\eta^2 + \beta^2}{\delta} \right). \quad (22)$$

Moreover, (i) bound (22) is tight when considered over all $\widehat{\mathcal{L}}$ that satisfy *Assumption 2* in the sense that $\exists \widehat{\mathcal{L}}$ such that (22) holds with equality, and (ii) $\gamma = \gamma_*$ is optimal in the sense that, without further assumptions on $\widehat{\mathcal{L}}$, γ_* minimizes a tight upper bound on $\kappa(\mathcal{P}_{\delta,\gamma})$, with $\gamma_* = \operatorname{argmin}_{\gamma \in (0, \infty)} \max_{\widehat{\mathcal{L}}} \kappa(\mathcal{P}_{\delta,\gamma})$.

Corollary 1 (Condition-number bounds, independent of $\widehat{\mathcal{L}}$). The maximum ℓ^2 condition number of the preconditioned operator (20) over all $\widehat{\mathcal{L}}$ that satisfy *Assumption 2*, is minimized over $\gamma \in (0, \infty)$ by

$$\gamma_* = \eta + \frac{\beta^2}{\eta}. \quad (23)$$

Furthermore, the maximum condition number of (20) when $\gamma = \gamma_*$ is tightly bounded for all $\widehat{\mathcal{L}}$ by

$$\kappa(\mathcal{P}_{\gamma_*}) \leq 1 + \frac{\beta^2}{2\eta^2}. \quad (24)$$

Proof. The preconditioned operator (20) is equivalent to the more general operator (21) analyzed in *Theorem 1* with $\delta = \eta$. Upon letting $\delta = \eta$, the value of γ_* (23) follows by definition from *Theorem 1* and the bound on $\kappa(\mathcal{P}_{\gamma_*})$ (24) follows from (22). \square

Table 1 provides condition number bounds from *Corollary 1* and (24) for Gauss, Radau IIA, and Lobatto IIIC Runge-Kutta methods.

Stages	2	3		4		5		
	$\lambda_{1,2}^\pm$	λ_1	$\lambda_{2,3}^\pm$	$\lambda_{1,2}^\pm$	$\lambda_{3,4}^\pm$	λ_1	$\lambda_{2,3}^\pm$	$\lambda_{4,5}^\pm$
Gauss	1.17	1.00	1.46	1.80	1.05	1.00	2.18	1.14
Radau IIA	1.25	1.00	1.65	2.11	1.06	1.00	2.60	1.16
Lobatto IIIC	1.50	1.00	2.11	2.76	1.07	1.00	3.44	1.19

Table 1: Bounds on $\kappa(\mathcal{P}_{\gamma_*})$ from *Corollary 1* and (24) for Gauss, Radau IIA, and Lobatto IIIC integration, with 2–5 stages. Each column within a given set of stages corresponds to either a real eigenvalue, $\lambda_1 = \eta$, or a conjugate pair of eigenvalues, e.g., $\lambda_{2,3}^\pm = \eta \pm i\beta$, of A_0^{-1} .

Remark 4 (Symmetric definite and skew symmetric operators). Using eigenvalue analysis, it is possible to derive tight upper bounds on the condition number of (20) for all $\gamma \in (0, \infty)$ when $\widehat{\mathcal{L}}$ is symmetric negative semi-definite (SNSD) or skew symmetric (SS) (see [4] for related derivations). These tight upper bounds achieve equality for

all $\gamma \in (0, \infty)$ as the spectrum of $\widehat{\mathcal{L}}$ becomes dense in $[0, \infty)$ for SNSD $\widehat{\mathcal{L}}$, and dense in $(-\infty, \infty)$ for SS $\widehat{\mathcal{L}}$. In each case, the tight upper bounds are minimized over all $\gamma \in (0, \infty)$ when $\gamma = \gamma_*$, for γ_* given by (23), which is perhaps unsurprising given [Corollary 1](#). At the minimum $\gamma = \gamma_*$, the tight bound for the SNSD case is

$$\kappa(\mathcal{P}_{\gamma_*}) \leq \frac{1}{2} \left(1 + \sqrt{1 + \beta^2/\eta^2} \right),$$

and for the SS case it is equal to that in (24), due to the general bound of (24) achieving equality for a matrix $\widehat{\mathcal{L}}$ having eigenvalues $\{0, \pm i\sqrt{\eta^2 + \beta^2}\}$.

4.2 $\widehat{\mathcal{L}}_1 \neq \widehat{\mathcal{L}}_2$

This section considers the more general case of $\widehat{\mathcal{L}}_1 \neq \widehat{\mathcal{L}}_2$. Similar to [Theorem 1](#) and [Corollary 1](#), [Theorem 2](#) derives an upper bound on condition number of the right-preconditioned Schur complement as in (19), with γ_* as in (23).² The proof we derived requires an additional assumption regarding the relation of $\widehat{\mathcal{L}}_1$ and $\widehat{\mathcal{L}}_2$, namely that $\langle \widehat{\mathcal{L}}_1 \mathbf{w}, \widehat{\mathcal{L}}_2 \mathbf{w} \rangle \geq 0$. It is worth pointing out that we do not believe this assumption is necessary for the result to hold, particularly for the discretization of PDEs where $\widehat{\mathcal{L}}_1$ and $\widehat{\mathcal{L}}_2$ are structured and correspond to the same operator evaluated at successive Runge-Kutta stages. However, we have been unable to find a more general proof that does not use this assumption. Under this additional assumption, [Theorem 2](#) proves that the condition number of the preconditioned Schur complement for $\widehat{\mathcal{L}}_1 \neq \widehat{\mathcal{L}}_2$ is at most $2 \times$ larger than as proven for $\widehat{\mathcal{L}}_1 = \widehat{\mathcal{L}}_2$ in [Corollary 1](#). By [Table 1](#), it is clear the conditioning is still bounded by a small, order-one constant, even for 10th-order integration.

Theorem 2 (Conditioning of preconditioned operator). *Suppose Assumptions 1 and 2 hold, that is, $\eta > 0$ and $W(\widehat{\mathcal{L}}_1), W(\widehat{\mathcal{L}}_2) \leq 0$. Additionally, assume that $\langle \widehat{\mathcal{L}}_1 \mathbf{w}, \widehat{\mathcal{L}}_2 \mathbf{w} \rangle \geq 0$. Let \mathcal{P}_γ denote the right-preconditioned Schur complement (19), with $\gamma = \gamma_* := \frac{\eta^2 + \beta^2}{\eta}$ as in (23). Let $\kappa(\mathcal{P}_{\gamma_*})$ denote the two-norm condition number of \mathcal{P}_{γ_*} . Then*

$$\kappa(\mathcal{P}_{\gamma_*}) \leq 2 + \frac{\beta^2}{\eta^2}. \quad (25)$$

Proof. See [Appendix A](#). □

5 Algorithm description

Before moving on to discuss DAEs and numerical results, here we provide a comprehensive description of the IRK algorithm. First, we introduce some practical notation and the operators that would arise in practice (rather than the analysis tools of scaling by M^{-1}), and then the algorithm is given in [Algorithm 1](#). To simplify the presentation, assume that s is even, and A_0^{-1} has $s/2$ complex-conjugate eigenvalue pairs $\{\eta_i \pm i\beta_i\}_{i=1}^{s/2}$; it is straightforward to modify the following description for the alternative case of one real-valued eigenvalue.

Recall that previously we introduced the operator $\widehat{\mathcal{L}} = \delta t M^{-1} \mathcal{L}$ to simplify notation. In practice, rather than solving an approximate Jacobian system that involves this operator, we solve one that has first been scaled by $I \otimes M$. That is, we invert the approximate Jacobian $R_0 \otimes M - (I \otimes M) \widetilde{P}$ rather than $R_0 \otimes I - \widetilde{P}$ which is based on (11). Consider decomposing the approximate Jacobian $R_0 \otimes M - (I \otimes M) \widetilde{P}$ into the sum

²Considering right preconditioning is a theoretical tool to facilitate the proof of [Theorem 2](#), but in practice left and right preconditioning have both proven effective.

of a block diagonal matrix \mathcal{D} having 2×2 blocks, and a strictly block upper triangular matrix \mathcal{U} having 2×2 blocks:

$$R_0 \otimes M - (I \otimes M)\tilde{P} = \mathcal{D} + \mathcal{U} = \begin{bmatrix} \mathcal{D}_1 & \mathcal{U}_{1,2} & \mathcal{U}_{1,3} & \cdots & \mathcal{U}_{1,s/2} \\ \mathbf{0} & \mathcal{D}_2 & \mathcal{U}_{2,3} & \cdots & \mathcal{U}_{2,s/2} \\ & \mathbf{0} & \ddots & & \vdots \\ & & \ddots & \ddots & \vdots \\ & & & \mathbf{0} & \mathcal{D}_{s/2} \end{bmatrix}. \quad (26)$$

The particular structure of these matrices is governed by which of the Newton-like methods is used. For Newton-like methods 0, 1, and 2, \mathcal{U} is equal to the strictly (block) upper triangular component of $R_0 \otimes M$, while for Newton-like method 3 it is equal to the strictly (block) upper triangular component of $R_0 \otimes M - (Q_0^T \otimes I)\text{diag}(\delta t \mathcal{L}_1, \dots, \delta t \mathcal{L}_s)(Q_0 \otimes I)$ (see (12)). The structure of the diagonal blocks \mathcal{D}_i in (26) are equal to those in (14) with each row simply scaled by M :

$$\mathcal{D}_i := \begin{bmatrix} \eta_i M - \delta t e_{2i-1,2i-1}^T \mathcal{L} & \phi_i M - \delta t e_{2i-1,2i}^T \mathcal{L} \\ -\frac{\beta_i^2}{\phi_i} M - \delta t e_{2i,2i-1}^T \mathcal{L} & \eta_i M - \delta t e_{2i,2i}^T \mathcal{L} \end{bmatrix}, \quad i \in \{1, \dots, s/2\}, \quad (27)$$

where $e_{a,b}^T \mathcal{L} \approx d_{a,b}^T \mathcal{L}$, with the particular approximation governed by which of the Newton-like methods is used.

Recall that a lower triangular, Schur-complement-based preconditioner (16) is used to precondition the Krylov solution of the blocks (27). In general, after scaling by M , this preconditioner takes the form

$$L_{P_i} := \begin{bmatrix} \eta_i M - \delta t e_{2i-1,2i-1}^T \mathcal{L} & \mathbf{0} \\ -\frac{\beta_i^2}{\phi_i} M - \delta t e_{2i,2i-1}^T \mathcal{L} & \gamma_i M - \delta t e_{2i,2i}^T \mathcal{L} \end{bmatrix}^{-1}. \quad (28)$$

Importantly, when computing the action of this preconditioner at every Krylov iteration, the exact inverses of the inner blocks are approximated with an inexact preconditioner. Recall here that γ_i is some constant, for example, $\gamma_i = \eta_i$ (the naive choice), or $\gamma_i = \eta_i + \beta_i^2/\eta_i$ (the optimal choice). In Line 9 of Algorithm 1, the syntax $\mathbf{x} \leftarrow \text{krylov}(A, \mathbf{b}, B)$ means to apply a Krylov solver the system $A\mathbf{x} = \mathbf{b}$ that is left or right preconditioned by $B \approx A^{-1}$.

6 Differential algebraic equations

This section considers differential algebraic equations (DAEs) that result from the spatial discretization of a time-dependent PDE with an algebraic (non-time-dependent) constraint. DAEs account for many interesting physical problems, with obvious examples including the many variations in incompressible flow that arise in fluid dynamics and plasma physics. Special treatment is also required for the time integration of DAEs, and this section discusses how to extend methods developed in this paper to DAEs.

DAEs arising from numerical PDEs take the general form

$$\begin{aligned} M\mathbf{u}_t &= \mathcal{N}(\mathbf{u}, \mathbf{w}, t), \\ \mathbf{0} &= \mathcal{G}(\mathbf{u}, \mathbf{w}, t), \end{aligned} \quad (29)$$

where M is a mass matrix and \mathcal{N} and \mathcal{G} nonlinear functions of the time-dependent variable, \mathbf{u} , the constraint variable, \mathbf{w} , and time. Time propagation using Runge-Kutta

Algorithm 1 Advance \mathbf{u}_n to \mathbf{u}_{n+1} using Newton-like solve on stage equations (3): $\mathbf{f}(\mathbf{k}) = \mathbf{0}$, where $\mathbf{k} = (\mathbf{k}_1, \dots, \mathbf{k}_s)$. Assume s even, and A_0^{-1} has $s/2$ complex-conjugate eigenvalue pairs.

```

// Define  $\mathbf{f}^{(\ell)} := \mathbf{f}(\mathbf{k}^{(\ell)})$ 
1:  $\ell \leftarrow 0$  ▷ Nonlinear iteration index
2: Initialize  $\mathbf{k}^{(\ell)}$  with initial guess for  $\mathbf{k}$ 
// Nonlinear iterations
3: while  $\|\mathbf{f}^{(\ell)}\|$  larger than tolerance do
    // Solve  $(\mathcal{D} + \mathcal{U})(R_0^{-1}Q_0^T \otimes I)\delta\mathbf{k} = -(\mathcal{Q}_0^T \otimes I)\mathbf{f}^{(\ell)}$  by solving
    //  $(\mathcal{D} + \mathcal{U})\widehat{\delta\mathbf{k}} = -\widehat{\mathbf{f}}^{(\ell)}$  via block backward substitution
4:  $\widehat{\mathbf{f}}^{(\ell)} \leftarrow (\mathcal{Q}_0^T \otimes I)\mathbf{f}^{(\ell)}$  ▷ Scale RHS vector
5: for  $i = s/2 \rightarrow 1$  do ▷ Solve for  $\widehat{\delta\mathbf{k}}_{2i-1}, \widehat{\delta\mathbf{k}}_{2i}$ 
     $\begin{bmatrix} \mathbf{z}_{2i-1} \\ \mathbf{z}_{2i} \end{bmatrix} \leftarrow \begin{bmatrix} -\widehat{\mathbf{f}}_{2i-1}^{(\ell)} \\ -\widehat{\mathbf{f}}_{2i}^{(\ell)} \end{bmatrix}$  ▷ RHS of equations  $2i - 1$  and  $2i$ 
    // Subtract previously computed solutions to RHS
7: if  $i < s/2$  then
     $\begin{bmatrix} \mathbf{z}_{2i-1} \\ \mathbf{z}_{2i} \end{bmatrix} \leftarrow \begin{bmatrix} \mathbf{z}_{2i-1} \\ \mathbf{z}_{2i} \end{bmatrix} - [\mathcal{U}_{i,i+1} \ \dots \ \mathcal{U}_{i,s/2}] \begin{bmatrix} \delta\mathbf{k}_{2i+1} \\ \delta\mathbf{k}_{2i+2} \\ \vdots \\ \delta\mathbf{k}_{s-1} \\ \delta\mathbf{k}_s \end{bmatrix}$ 
    // Solve  $2 \times 2$  system on diagonal
9:  $\begin{bmatrix} \delta\mathbf{k}_{2i} \\ \delta\mathbf{k}_{2i-1} \end{bmatrix} \leftarrow \text{krylov}\left(\mathcal{D}_i, \begin{bmatrix} \mathbf{z}_{2i} \\ \mathbf{z}_{2i-1} \end{bmatrix}, L_{P_i}\right)$ 
10:  $\delta\mathbf{k} \leftarrow (Q_0 R_0 \otimes I)\delta\mathbf{k}$  ▷ Scale solution by inverse of  $R_0^{-1}Q_0^T \otimes I$ 
11:  $\mathbf{k}^{(\ell+1)} \leftarrow \mathbf{k}^{(\ell)} + \delta\mathbf{k}$  ▷ Update stage vectors
12:  $\ell \leftarrow \ell + 1$  ▷ Update nonlinear iteration index
// Nonlinear iteration has converged
13:  $\mathbf{k} \leftarrow \mathbf{k}^{(\ell+1)}$  ▷ Accept Newton solution
14:  $\mathbf{u}_{n+1} \leftarrow \mathbf{u}_n + \delta t \sum_{i=1}^s b_i \mathbf{k}_i$  ▷ IRK solution at  $t_{n+1}$  using (2)

```

integration then takes a similar form to (2), where

$$\mathbf{u}_{n+1} = \mathbf{u}_n + \delta t \sum_{i=1}^s b_i \mathbf{k}_i, \quad \mathbf{w}_{n+1} = \mathbf{w}_n + \delta t \sum_{i=1}^s b_i \boldsymbol{\ell}_i,$$

and stage vectors $\{\mathbf{k}_i\}$ and $\{\boldsymbol{\ell}_i\}$ are given as the solution of the nonlinear set of equations [7, Ch. 4]

$$\begin{aligned} \mathcal{N}_i &:= M\mathbf{k}_i - \mathcal{N} \left(\mathbf{u}_n + \delta t \sum_{j=1}^s a_{ij} \mathbf{k}_j, \mathbf{w}_n + \delta t \sum_{j=1}^s a_{ij} \boldsymbol{\ell}_j, t_n + c_i \delta t \right) = \mathbf{0}, \\ \mathcal{G}_i &:= -\mathcal{G} \left(\mathbf{u}_n + \delta t \sum_{j=1}^s a_{ij} \mathbf{k}_j, \mathbf{w}_n + \delta t \sum_{j=1}^s a_{ij} \boldsymbol{\ell}_j, t_n + c_i \delta t \right) = \mathbf{0}. \end{aligned} \quad (30)$$

The linear case: To start, consider a linear set of DAEs, where (29) can be expressed as the linear set of equations

$$\begin{bmatrix} M\mathbf{u}_t \\ \mathbf{0} \end{bmatrix} = \begin{bmatrix} \mathcal{L}_u & \mathcal{L}_w \\ \mathcal{G}_u & \mathcal{G}_w \end{bmatrix} \begin{bmatrix} \mathbf{u} \\ \mathbf{w} \end{bmatrix} + \begin{bmatrix} \mathbf{f}(t) \\ \mathbf{g}(t) \end{bmatrix}. \quad (31)$$

Then, the equations defining stage vectors (30) can be expressed as a large block linear system,

$$\left(\begin{bmatrix} \begin{bmatrix} M & \mathbf{0} \\ \mathbf{0} & \mathbf{0} \end{bmatrix} & & & \\ & \ddots & & \\ & & \begin{bmatrix} M & \mathbf{0} \\ \mathbf{0} & \mathbf{0} \end{bmatrix} & \\ & & & \end{bmatrix} - \delta t \begin{bmatrix} a_{11} \begin{bmatrix} \mathcal{L}_u & \mathcal{L}_w \\ \mathcal{G}_u & \mathcal{G}_w \end{bmatrix} & \dots & a_{1s} \begin{bmatrix} \mathcal{L}_u & \mathcal{L}_w \\ \mathcal{G}_u & \mathcal{G}_w \end{bmatrix} \\ & \ddots & \ddots & \vdots \\ & & a_{s1} \begin{bmatrix} \mathcal{L}_u & \mathcal{L}_w \\ \mathcal{G}_u & \mathcal{G}_w \end{bmatrix} & \dots & a_{ss} \begin{bmatrix} \mathcal{L}_u & \mathcal{L}_w \\ \mathcal{G}_u & \mathcal{G}_w \end{bmatrix} \end{bmatrix} \right) \begin{bmatrix} \mathbf{k}_1 \\ \boldsymbol{\ell}_1 \\ \vdots \\ \mathbf{k}_s \\ \boldsymbol{\ell}_s \end{bmatrix} = \begin{bmatrix} \mathbf{f}_1 \\ \mathbf{g}_1 \\ \vdots \\ \mathbf{f}_s \\ \mathbf{g}_s \end{bmatrix}, \quad (32)$$

where $\mathbf{f}_i = (\mathbf{f}(t_i + c_i \delta t) + \mathcal{L}_u \mathbf{u}_n + \mathcal{L}_w \mathbf{w}_n)$ and $\mathbf{g}_i = (\mathbf{g}(t_i + c_i \delta t) + \mathcal{G}_u \mathbf{u}_n + \mathcal{G}_w \mathbf{w}_n)$. In this case, (32) can be reduced to the Kronecker-product form

$$\left(I \otimes \begin{bmatrix} M & \mathbf{0} \\ \mathbf{0} & \mathbf{0} \end{bmatrix} - \delta t A_0 \otimes \begin{bmatrix} \mathcal{L}_u & \mathcal{L}_w \\ \mathcal{G}_u & \mathcal{G}_w \end{bmatrix} \right) \mathbf{K} = \mathbf{F}.$$

The nonlinear case: Now consider general nonlinear DAEs (29) that arise in the context of numerical PDEs. Linearizing (30) results in a linear set of equations similar to (32), but with linearized operator that depends on stages. Similar to the nonlinear ODE case (see Section 1.1), it is generally the case that the 2×2 linearized operator is fixed for a given stage (i.e., block row of the matrix), a natural result of the chain rule applied to (30). Pulling out $A_0 \otimes I$ as in the ODE setting yields a block linear system of the form

$$\left(A_0^{-1} \otimes \begin{bmatrix} M & \mathbf{0} \\ \mathbf{0} & \mathbf{0} \end{bmatrix} - \delta t \begin{bmatrix} \begin{bmatrix} \mathcal{L}_u^{(1)} & \mathcal{L}_w^{(1)} \\ \mathcal{G}_u^{(1)} & \mathcal{G}_w^{(1)} \end{bmatrix} & & & \mathbf{0} \\ & \ddots & & \\ & & \begin{bmatrix} \mathcal{L}_u^{(s)} & \mathcal{L}_w^{(s)} \\ \mathcal{G}_u^{(s)} & \mathcal{G}_w^{(s)} \end{bmatrix} & \\ & & & \mathbf{0} \end{bmatrix} \right) (A_0 \otimes I) \begin{bmatrix} \mathbf{k}_1 \\ \boldsymbol{\ell}_1 \\ \vdots \\ \mathbf{k}_s \\ \boldsymbol{\ell}_s \end{bmatrix} = \begin{bmatrix} \mathbf{f}_1 \\ \mathbf{g}_1 \\ \vdots \\ \mathbf{f}_s \\ \mathbf{g}_s \end{bmatrix}. \quad (33)$$

Inverting (33) corresponds to the application of \mathcal{P}^{-1} in the nonlinear Richardson iteration (10) applied to solving the nonlinear stage equations (30). Note, in a nonlinear iteration, the operator in (33) is usually updated each iteration to reflect the latest nonlinear iterate.

Solving linear systems: Now, techniques developed in [Section 3](#) can be applied to solve or approximate (33) as a single step in the larger nonlinear iteration to solve (30). For DAEs, the 2×2 block systems that arise after applying the real Schur decomposition (as discussed in [Section 4](#)) are now 4×4 systems of the form

$$\begin{bmatrix} \eta M - \delta t \mathcal{L}_u^{(i)} & -\delta t \mathcal{L}_w^{(i)} & \phi M & \mathbf{0} \\ -\delta t \mathcal{G}_u^{(i)} & -\delta t \mathcal{G}_w^{(i)} & \mathbf{0} & \mathbf{0} \\ -\frac{\beta^2}{\phi} M & \mathbf{0} & \eta M - \delta t \mathcal{L}_u^{(i+1)} & -\delta t \mathcal{L}_w^{(i+1)} \\ \mathbf{0} & \mathbf{0} & -\delta t \mathcal{G}_u^{(i+1)} & -\delta t \mathcal{G}_w^{(i+1)} \end{bmatrix} \begin{bmatrix} \mathbf{k}_i \\ \boldsymbol{\ell}_i \\ \mathbf{k}_{i+1} \\ \boldsymbol{\ell}_{i+1} \end{bmatrix} = \begin{bmatrix} \mathbf{f}_i \\ \mathbf{g}_i \\ \mathbf{f}_{i+1} \\ \mathbf{g}_{i+1} \end{bmatrix}. \quad (34)$$

For index-1 DAEs, where the algebraic constraint can be formally eliminated from the problem (although it is often not practical to do so), [Assumption 2](#) naturally applies to the reduced time-dependent problem. Then, the block preconditioning techniques and theory developed in [Section 4](#) can be formally applied when the algebraic constraint is inverted to high accuracy within each preconditioner application. Inexact application of the constraint makes [Assumption 2](#) less certain, but for index-1 DAEs we expect the methods developed here to remain effective with approximate inner inverses.

In the more general setting, such as index-2 DAEs, preconditioning (34) and the corresponding Schur complement requires more problem-specific analysis than the theory developed for ODEs in [Section 4](#). In particular, [Assumption 2](#) does not necessarily hold for the larger linear system that includes time-dependent variables and constraints (the obvious example being indefinite saddle-point systems that often arise in incompressible fluid dynamics). However, [Section 7.2](#) considers a Picard iteration of incompressible Navier Stokes in vorticity-stream-function form (an index-1 DAE), where (34) can be reordered to be block triangular, and the theory and preconditioning developed in [Section 4](#) can be applied directly to the leading 2×2 block representing time-dependent variables (\mathbf{k}_i and \mathbf{k}_{i+1}).

7 Numerical results

In this section, we apply the solvers and preconditioners developed above to several fluid flow problems. The solvers and spatial discretizations were implemented using the MFEM finite element library [2]. All numerical results will use the constant $\gamma = \gamma_*$ (23) unless otherwise specified.

7.1 Compressible Euler & Navier–Stokes equations

Consider the compressible Navier–Stokes equations, given by

$$\frac{\partial \rho}{\partial t} + \frac{\partial}{\partial x_j} (\rho u_j) = 0, \quad (35)$$

$$\frac{\partial}{\partial t} (\rho u_i) + \frac{\partial}{\partial x_j} (\rho u_i u_j) + \frac{\partial p}{\partial x_i} = \frac{\partial \tau_{ij}}{\partial x_j} \quad \text{for } i = 1, 2, 3, \quad (36)$$

$$\frac{\partial}{\partial t} (\rho E) + \frac{\partial}{\partial x_j} (u_j (\rho E + p)) = -\frac{\partial q_j}{\partial x_j} + \frac{\partial}{\partial x_j} (u_i \tau_{ij}), \quad (37)$$

using the convention that repeated indices are implicitly summed. In the above, ρ is the density, u_i is the i th component of the velocity, and E is the total energy. The viscous stress tensor and heat flux are given by

$$\tau_{ij} = \mu \left(\frac{\partial u_i}{\partial x_j} + \frac{\partial u_j}{\partial x_i} - \frac{2}{3} \frac{\partial u_k}{\partial x_k} \delta_{ij} \right) \quad \text{and} \quad q_j = -\frac{\mu}{\text{Pr}} \frac{\partial}{\partial x_j} \left(E + \frac{p}{\rho} - \frac{1}{2} u_k u_k \right), \quad (38)$$

Table 2: Error and convergence rates for Euler vortex problem.

δt	Gauss 2		Gauss 4		Gauss 6	
	Error	Rate	Error	Rate	Error	Rate
2.50×10^{-2}	5.89×10^{-3}	—	5.29×10^{-4}	—	1.65×10^{-5}	—
1.25×10^{-2}	1.18×10^{-3}	2.32	2.75×10^{-5}	4.26	2.35×10^{-7}	6.14
6.25×10^{-3}	2.82×10^{-4}	2.07	1.64×10^{-6}	4.07	3.69×10^{-9}	5.99
	Radau 3		Radau 5		Radau 7	
2.50×10^{-2}	1.19×10^{-3}	—	8.48×10^{-5}	—	1.92×10^{-6}	—
1.25×10^{-2}	1.62×10^{-4}	2.88	2.78×10^{-6}	4.92	1.68×10^{-8}	6.84
6.25×10^{-3}	2.17×10^{-5}	2.90	9.23×10^{-8}	4.91	2.16×10^{-10}	6.28
	Lobatto 2		Lobatto 4		Lobatto 6	
2.50×10^{-2}	2.45×10^{-3}	—	2.76×10^{-4}	—	1.30×10^{-5}	—
1.25×10^{-2}	1.12×10^{-3}	1.13	2.39×10^{-5}	3.53	2.52×10^{-7}	5.69
6.25×10^{-3}	3.93×10^{-4}	1.88	2.39×10^{-6}	3.67	4.42×10^{-9}	5.83

where μ is the viscosity coefficient, and Pr is the Prandtl number. We assume that the pressure p is given by the equation of state $p = (\gamma - 1)\rho(E - \frac{1}{2}u_k u_k)$, where $\gamma = 1.4$ is the adiabatic gas constant. We obtain the compressible Euler equations from equations (35–37) by setting the viscosity coefficient $\mu = 0$. For the viscous problems, we introduce an additional isentropic assumption of the form $p = K\rho^\gamma$, for a given constant K . This simplification is described in [23] and results in a reduced system of equations.

7.1.1 Isentropic Euler vortex

For a first test case, we consider the model problem of an inviscid isentropic vortex [44, 51]. The spatial domain is $\Omega = [0, 20] \times [-7.5, 7.5]$. The vortex, initially centered at (x_0, y_0) , is advected with the freestream velocity at an angle of θ . The exact solution for this problem is given analytically by

$$u = u_\infty \left(\cos(\theta) - \frac{\epsilon((y - y_0) - \bar{v}t)}{2\pi r_c} e^{\frac{f(x,y,t)}{2}} \right), \quad \rho = \rho_\infty \left(1 - \frac{\epsilon^2(\gamma - 1)M_\infty^2}{8\pi^2} e^{f(x,y,t)} \right)^{\frac{1}{\gamma-1}},$$

$$v = u_\infty \left(\sin(\theta) - \frac{\epsilon((x - x_0) - \bar{u}t)}{2\pi r_c} e^{\frac{f(x,y,t)}{2}} \right), \quad p = p_\infty \left(1 - \frac{\epsilon^2(\gamma - 1)M_\infty^2}{8\pi^2} e^{f(x,y,t)} \right)^{\frac{\gamma}{\gamma-1}}.$$

In the above, $f(x, y, t) = (1 - ((x - x_0) - \bar{u}t)^2 - ((y - y_0) - \bar{v}t)^2)/r_c^2$, and M_∞, ρ_∞ , and p_∞ are the freestream Mach number, density, and pressure, respectively. The freestream velocity is given by $(\bar{u}, \bar{v}) = u_\infty(\cos(\theta), \sin(\theta))$. The parameters for this test case are given by $\epsilon = 15$, $r_c = 1.5$, $M_\infty = 0.5$, $\theta = \arctan(1/2)$, $u_\infty = 1$, $\rho_\infty = 1$. We discretize this problem using a high-order DG method with Roe numerical fluxes [40]. The spatial domain is discretized with a structured triangular mesh with 532 elements. The DG finite element space is chosen to use piecewise polynomials of degree 4.

We first verify the temporal order of accuracy by fixing the spatial discretization computing a baseline solution using an explicit fourth-order Runge–Kutta method with $\delta t = 5 \times 10^{-5}$. Then, the solutions computed using the implicit Runge–Kutta methods are compared to the baseline solution to estimate the observed order of convergence for these problems. The results are presented in Table 2. The expected rates of convergence are observed for Gauss, Radau, and Lobatto methods, of orders 2 through 7.

We next study the effectiveness of the solvers and preconditioners for the resulting algebraic systems of equations. We make use of an element-wise block ILU preconditioner

Table 3: Convergence results for Euler vortex test case, showing Newton iterations required for a single time step with $\delta t = 2 \times 10^{-2}$, and total preconditioner applications per time step.

Order	SDIRK				Gauss				
	1	2	3	4	2	4	6	8	10
Newton its.	3	3	3	3	3	3	5	5	5
Precond. applications	20	26	45	59	15	36	103	162	169

Order	Radau				Lobatto			
	3	5	7	9	2	4	6	8
Newton its.	3	5	5	5	3	8	5	6
Precond. applications	44	121	168	205	66	225	210	292

Table 4: Convergence results for Euler vortex test case. Average Krylov iterations are shown for 2×2 systems, denoted “Kry.”.

Order	Gauss				Radau				Lobatto			
	4	6	8	10	3	5	7	9	2	4	6	8
Newton its.	3	5	5	5	3	5	5	5	3	8	5	6
Kry. ($\gamma = \eta$)	7.7	12.6	12.5	14.9	9.0	16.8	15.5	20.6	13.7	24.4	25.3	35.2
Kry. ($\gamma = \gamma_*$)	6.0	8.4	8.1	7.6	7.3	10.2	8.4	9.3	11.0	12.0	10.5	11.2

with minimum discarded fill ordering that has been shown to be effective for convection-dominated fluid problems [36]. In Table 3, we present the number of nonlinear iterations required to converge with a representative time step of $\delta t = 2 \times 10^{-2}$, together with the total number of preconditioner applications in one step. In these tests, a relative nonlinear tolerance of 10^{-9} was used, and each linear system was solved using GMRES with a relative tolerance of 10^{-5} . Each Krylov iteration for the SDIRK methods corresponds to a single preconditioner application. For the fully implicit IRK methods, one Krylov iteration for a 1×1 system corresponds to one preconditioner application, whereas for a 2×2 system, one Krylov iteration corresponds to two preconditioner applications. We note that the second- and fourth-order Gauss methods require fewer total preconditioner applications when compared with the equal-order SDIRK methods. Similarly, the third-order Radau IIA method requires one fewer preconditioner application when compared with the third-order SDIRK method. The Lobatto methods are significantly more expensive than the equal-order Gauss methods for this test case.

Finally, in Section 7.1.1 we study the effect of the choice of the coefficient γ appearing in the linear preconditioner (16). We compare the naive choice of $\gamma = \eta$ to the improved choice of $\gamma = \gamma_*$, where γ_* is as in Corollary 1. This choice is shown to be optimal in the case where $\hat{\mathcal{L}}_1 = \hat{\mathcal{L}}_2$. Although this assumption does not hold in this case because the equations are fully nonlinear, we still observe significantly improved iteration counts with this choice of γ , consistent with Theorem 2.

7.1.2 Flow over NACA airfoil

As a more challenging test case, we consider the Reynolds number 40,000 flow over a NACA0012 airfoil. The angle of attack is 30° and the farfield Mach number is 0.1.

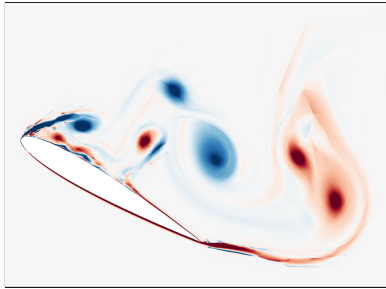


Figure 1: Snapshot of vorticity for Reynolds 40,000 flow over NACA airfoil.

The domain is discretized using a triangular mesh with 3154 elements, and the spatial discretization is a high-order discontinuous Galerkin method using compact stencils for the second order (viscous) terms with polynomial degree $p = 3$ [35]. No-slip boundary conditions are enforced at the surface of the airfoil, and farfield boundary conditions at all other domain boundaries. The main challenge associated with this problem is the resolution of the thin boundary layer at the surface of the airfoil that results from the no-slip condition. This boundary layer is resolved using a layer of anisotropically stretched elements near the surface of the airfoil. These elements result in a highly restrictive CFL stability condition, motivating the use of implicit time integration for this problem. A time accurate time step of $\delta t = 5 \times 10^{-2}$ is chosen for this problem. This time step is several orders of magnitude larger than the largest stable explicit time step. The number of nonlinear iterations and preconditioner applications required for convergence are shown in Table 5. The nonlinear tolerance was chosen to be 10^{-9} , and each linear system was solved using GMRES with a relative tolerance of 10^{-5} . As in the previous case, each Krylov iteration for the SDIRK methods corresponds to a single preconditioner application. For the IRK methods, one Krylov iteration for a 1×1 system corresponds to one preconditioner application, whereas for a 2×2 system, one Krylov iteration corresponds to two preconditioner applications. As we observed in the case of the Euler vortex, the Gauss and Radau fully implicit Runge–Kutta methods of 2, 3, and 4 converge with fewer total preconditioner applications than the equal-order SDIRK method.

Additionally, we use this test case to compare four potential solver strategies, corresponding to those enumerated in Section 3.2. The first solver (Solver 0) uses a simplified Newton nonlinear iteration, where the Jacobian matrix from the first stage is used for all stages. This has the advantage that the number of Jacobian matrix assemblies per nonlinear iteration is reduced; however, in general, the quadratic convergence of Newton’s method is not maintained, typically resulting in an increased number of nonlinear iterations. The remaining solvers (Solvers 1, 2, and 3) use exactly computed Jacobian matrices at all temporal stages, and each solver corresponds to a different approximation $\tilde{P} \approx \hat{P}$, as described in Section 3.2. With increasing quality of the approximation, we expect the solver to converge more rapidly, however each iteration will generally be more expensive to compute. In Figure 2 we compare the number of nonlinear iterations, number of matrix-vector products (determined by the convergence of the Krylov solvers), number of Jacobian assemblies, and total wall-clock runtime for these solver configurations (runtimes are measured using a Linux workstation with 16 Intel Xeon Gold 2.10 GHz CPUs and 124 GB memory). From these results, we see that for this problem, the nonlinear iterations based on better approximations lead to overall faster runtimes, despite the higher per-iteration cost. However, we note that this performance is often problem-dependent. In particular, for smaller time steps and less stiff problems, the simplified Newton method can be more efficient because few Jacobian assemblies are required, and the increase in nonlinear iterations over Solvers 1, 2, and 3 is typically

Table 5: Nonlinear iterations and preconditioner applications for the NACA airfoil test case, with time step $\delta t = 5 \times 10^{-2}$, using Newton-like Solver 3 with a relative tolerance of 10^{-9} .

Order	SDIRK				Gauss				
	1	2	3	4	2	4	6	8	10
Newton its.	5	5	5	5	5	5	8	8	8
Precond. applications	173	200	359	481	128	244	557	732	830

Order	Radau				Lobatto		
	3	5	7	9	2	6	8
Newton its.	5	9	9	9	5	15	17
Precond. applications	314	728	926	1061	454	1670	1995

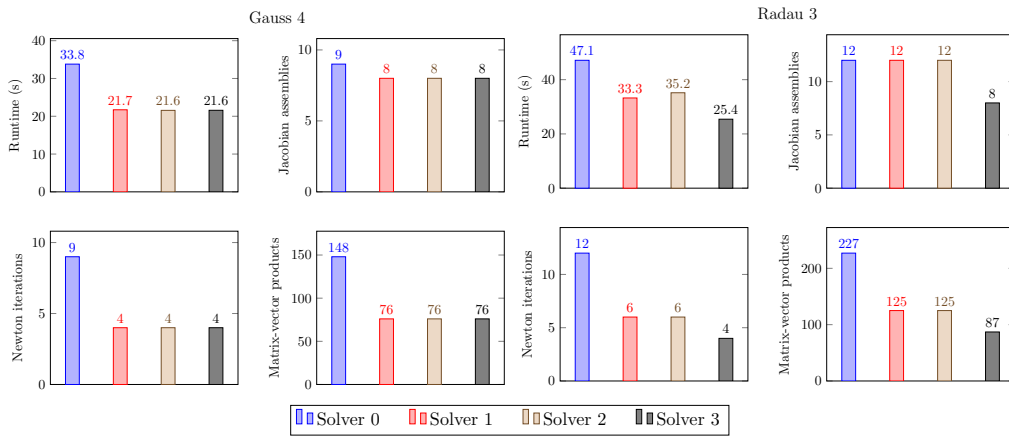


Figure 2: Performance for four solver configurations on the NACA test case with $\delta t = 2 \times 10^{-2}$.

less significant.

7.2 Incompressible Euler & Navier–Stokes in vorticity-streamfunction form

As an example of an index-1 DAE, we consider the vorticity-streamfunction formulation of the 2D incompressible Euler equations [28], given by

$$\frac{\partial \omega}{\partial t} + \nabla \cdot (\mathbf{u}\omega) = 0, \quad \text{and} \quad \Delta \psi = \omega, \quad (39)$$

where the velocity \mathbf{u} is defined by $\mathbf{u} = \nabla^\perp \psi$, for $\nabla^\perp = (-\partial_y, \partial_x)$. Here, ω is the vorticity, and ψ is a scalar field known as the streamfunction, which is used to naturally enforce the divergence-free constraint on the velocity. Note that this formulation can be easily extended to the 2D incompressible Navier–Stokes equations with the addition of a viscosity term, replacing left left-hand term of equation (39) with $\frac{\partial \omega}{\partial t} + \nabla \cdot (\mathbf{u}\omega) = \frac{1}{\text{Re}} \Delta \omega$, where Re is the Reynolds number. For a fixed velocity \mathbf{u} , the left-hand term in equation (39) is a scalar advection equation for ω , which we discretize using an upwind discontinuous Galerkin method. If the streamfunction ψ is in H^1 , then the velocity $\mathbf{u} = \nabla^\perp \psi$ is automatically continuous across element interfaces, and therefore

the standard upwind numerical flux is well-defined. We therefore discretize $\Delta\psi$ using a standard H^1 -conforming finite element method. Equal-order finite element spaces are chosen for ω and ψ . In the case of the Navier–Stokes equations, we discretize the viscous term added to the right-hand side, $\frac{1}{\text{Re}}\Delta\omega$, using a standard interior penalty DG method [3].

After performing the discretization, this system of equations can be written as

$$\begin{bmatrix} M_{\text{dg}}\omega_t \\ 0 \end{bmatrix} = \begin{bmatrix} K(\psi) & 0 \\ M_{\text{mix}} & A \end{bmatrix} \begin{bmatrix} \omega \\ \psi \end{bmatrix}, \quad (40)$$

where M_{dg} represents the DG mass matrix, M_{mix} is the mixed DG- H^1 mass matrix, $K(\psi)$ is the discretized advection (or advection–diffusion) operator (depending the velocity \mathbf{u} as a function of ψ), and A is the H^1 -conforming diffusion operator. A Picard linearization of (40) will result in a block-triangular system that is of the same form as (40), but using an iteratively lagged advection operator. We use nonlinear method (1) from Section 3.2, where we lump the sum of operators on diagonal blocks to the dominant operator and ignore non-identity off-diagonal coupling. For this problem, tests indicated that including additional diagonal terms or off-diagonal coupling (as in methods (2) and (3)) requires slightly longer wall-clock times and do not offer significant reduction in nonlinear iterations. Then, in the notation of Section 6, we have $\mathcal{L}_u^{(i)} = K(\psi^{(i)})$, $\mathcal{L}_w = 0$, $\mathcal{G}_u = M_{\text{mix}}$, and $\mathcal{G}_w = A$. The resulting 4×4 block system that arises from IRK integration has the form

$$\begin{bmatrix} \eta M_{\text{dg}} - \delta t K^{(i)} & \mathbf{0} & \phi M_{\text{dg}} & \mathbf{0} \\ -\delta t M_{\text{mix}} & -\delta t A & \mathbf{0} & \mathbf{0} \\ -\frac{\beta^2}{\phi} M_{\text{dg}} & \mathbf{0} & \eta M_{\text{dg}} - \delta t K^{(i+1)} & \mathbf{0} \\ \mathbf{0} & \mathbf{0} & -\delta t M_{\text{mix}} & -\delta t A \end{bmatrix} \begin{bmatrix} \omega_i \\ \psi_i \\ \omega_{i+1} \\ \psi_{i+1} \end{bmatrix} = \begin{bmatrix} \mathbf{f}_i \\ \mathbf{g}_i \\ \mathbf{f}_{i+1} \\ \mathbf{g}_{i+1} \end{bmatrix}. \quad (41)$$

We consider two types of preconditioners for this system. The first is the block-triangular preconditioner described in Section 4. In this case, the Schur complement is approximated using (18), and the diagonal blocks are replaced by the appropriate preconditioners. An alternative preconditioner is obtained by noticing that this system can be reordered to obtain the block-triangular system

$$\begin{bmatrix} \eta M_{\text{dg}} - \delta t K^{(i)} & \phi M_{\text{dg}} & \mathbf{0} & \mathbf{0} \\ -\frac{\beta^2}{\phi} M_{\text{dg}} & \eta M_{\text{dg}} - \delta t K^{(i+1)} & \mathbf{0} & \mathbf{0} \\ -\delta t M_{\text{mix}} & \mathbf{0} & -\delta t A & \mathbf{0} \\ \mathbf{0} & -\delta t M_{\text{mix}} & \mathbf{0} & -\delta t A \end{bmatrix} \begin{bmatrix} \omega_i \\ \omega_{i+1} \\ \psi_i \\ \psi_{i+1} \end{bmatrix} = \begin{bmatrix} \mathbf{f}_i \\ \mathbf{f}_{i+1} \\ \mathbf{g}_i \\ \mathbf{g}_{i+1} \end{bmatrix}. \quad (42)$$

This block-triangular system can be solved using forward-substitution, first solving the leading 2×2 block for the time-dependent variables, and then solving two (independent) Poisson problems for the algebraic constraints (i.e. the streamfunctions).

Each of these approaches require preconditioning/inverting the diagonal blocks in (41)/(42). Poisson problems are solved with optimal complexity using AMG preconditioners. The advection diffusion equations defining vorticity are preconditioned using nonsymmetric AMG based on approximate ideal restriction (AIR) [30, 31]. The leading 2×2 time-dependent vorticity equations are preconditioned using the block-triangular preconditioners described in Section 4, coupled with AIR preconditioning for individual systems. For the block triangular variation (42), the 2×2 diagonal blocks are solved to high precision, while preconditioning diagonal blocks in (41) consists of *one* AIR or AMG iteration. All linear and nonlinear iterations are solved to relative residual tolerance of 10^{-9} , typically yielding an absolute tolerance $\sim \mathcal{O}(10^{-12})$.

To study the effectiveness of these preconditioners, we consider the double shear layer problem [5]. The domain is taken to be the square $[0, 2\pi] \times [0, 2\pi]$, and periodic

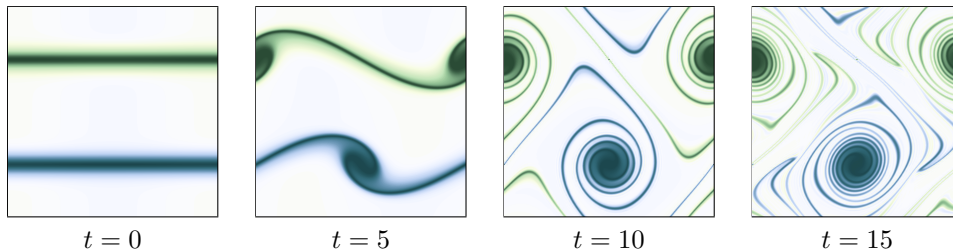


Figure 3: Time evolution of vorticity for the double shear layer problem.

boundary conditions are enforced at the domain boundaries. The initial condition is given by

$$\omega(x, y, 0) = \begin{cases} \delta \cos(x) - \frac{1}{\rho} \operatorname{sech}^2((y - \pi/2)/\rho) & y \leq \pi, \\ \delta \cos(x) + \frac{1}{\rho} \operatorname{sech}^2((3\pi/2 - y)) & y > \pi. \end{cases}$$

This test case is well-suited for high-order methods because the solution quickly develops small-scale features, as shown in [Figure 3](#). We use finite element spaces with polynomial degree $p = 3$, mesh spacing $h = 0.0025$, and choose a time step of $\delta t = 10^{-2}$ for all RK schemes to consider scalability in integration order for fixed δt . [Table 6](#) shows the total number of preconditioner applications required per time step with Reynolds number $\operatorname{Re} = 10$. Rows indicated “Prec. applications” correspond to [\(41\)](#), and each preconditioner application is defined as preconditioning a 2×2 block over $[\omega_i, \psi_i]$ with one AIR iteration and one AMG iteration (one for each diagonal block). The block triangular variation [\(42\)](#) does a block forward solve on [\(42\)](#), and [Table 6](#) presents the total number of AIR and AMG iterations required for the forward solve, summed over all nonlinear iterations. Note, because the time-dependent and algebraic blocks are solved separately in this case, the number of AIR iterations (to solve for the vorticity) and AMG iterations (to solve for the streamfunction) are not equal. These results were run on 288 cores on the Quartz machine at Lawrence Livermore National Laboratory.

Table 6: Preconditioner applications for the double shear layer test case, with third-order finite elements, mesh spacing $h = 0.0025$, time step $\delta t = 10^{-2}$, and $\operatorname{Re} = 10$. One “Prec. application” corresponds to one AIR iteration and one AMG iteration.

		SDIRK				Gauss				
		1	2	3	4	2	4	6	8	10
(41)	Prec. applications	127	141	322	365	78	161	218	287	333
(42)	AIR iterations	127	141	322	365	78	365	538	731	1064
	AMG iterations	127	141	322	365	78	368	562	766	1204

		Radau				Lobatto			
		3	5	7	9	2	4	6	8
(41)	Prec. applications	237	232	299	490	217	234	311	375
(42)	AIR iterations	451	603	841	989	421	697	2013	1405
	AMG iterations	432	566	819	980	350	670	1580	1227

Note from [Table 6](#) that the second and fourth order Gauss methods are significantly more efficient than the corresponding equal-order SDIRK methods in terms of total number of preconditioner applications, while the *10th-order* Gauss method requires approximately as many (in fact, slightly less) preconditioner applications per time step as

the fourth-order SDIRK method. In all cases, the triangular nonlinear preconditioning (42) requires many more iterations than the more general approach following the development in this paper (41). This is largely because the linear preconditioning ends up being more efficient when applied to the full system (41), rather than the reordered system in (42). Moreover, linear iteration counts are almost equal for nonlinear methods 1, 2, and 3 (results are not shown for sake of space) from Section 3.2, indicating that linear conditioning theory developed in Section 4.2 for systems that arise from nonlinear methods (1) and (2) yields robust preconditioners for method (3) as well.

Table 7 demonstrates that the proposed methods are also robust across Reynolds number, showing similar results as in Table 6, for the preconditioning in (41) with Reynolds number 25,000. As before, Gauss methods require roughly half the preconditioner applications as required by equal order SDIRK methods, while 4th-order SDIRK requires almost as many preconditioner applications as 10th-order Gauss, and more than 8th-order Gauss and 7th-order Radau IIA.

Table 7: Preconditioner applications for the double shear layer test case, with third-order finite elements, mesh spacing $h = 0.0025$, time step $\delta t = 10^{-2}$, and $\text{Re} = 25,000$. One ‘‘Prec. application’’ corresponds to one AIR iteration and one AMG iteration.

		SDIRK				Gauss				
Order		1	2	3	4	2	4	6	8	10
(41)	Prec. applications	41	72	113	177	37	75	118	163	194

		Radau				Lobatto			
Order		3	5	7	9	2	4	6	8
(41)	Prec. applications	81	123	165	206	91	130	173	220

To assess the accuracy of IRK methods applied to this problem, we consider the integration of the double shear layer problem over a longer time interval of $[0, 10]$. We choose a Reynolds number of 100, and compute a reference solution by applying explicit 6th-order SDIRK integration with a small time step of $\delta t = 10^{-4}$. We then apply IRK methods with large time steps of $\delta t \in \{0.4, 0.2, 0.1\}$ and observe the orders of convergence in Table 8. As a consequence of the nonlinear solver tolerance of 10^{-11} , the observed order of convergence is reduced for the highest order methods and the refinement $\delta t = 0.2 \mapsto \delta t = 0.1$. Nevertheless, we observe that each of the methods indeed yield high-order accuracy using very large time steps, in most cases just under their formal order of accuracy. Moreover, the leading error constants also appear to be small, given we can obtain accuracy on the order of $10^{-9} - 10^{-10}$ with a step size of $\delta t = 0.2$. Similar results have been observed on the Taylor Green vortex problem; here we use the double shear layer problem to demonstrate high-order accuracy on a problem with more interesting long-term dynamics.

8 Conclusions

This paper introduces a theoretical and algorithmic framework for the fast, parallel solution of fully implicit Runge-Kutta methods in numerical PDEs. Multiple approximate linearizations are developed, and linear algebra theory is derived to guarantee fast and effective block preconditioning techniques for the linearized systems, guaranteeing a preconditioned Schur complement with condition number bounded by a small order-one constant, and only requiring standard preconditioners as would be used for backward

Table 8: Error and convergence rates for double shear layer problem with Re= 10.

δt	Gauss 4		Gauss 6		Gauss 8	
	Error	Rate	Error	Rate	Error	Rate
0.4	1.98×10^{-3}	—	1.59×10^{-4}	—	4.13×10^{-5}	—
0.2	1.30×10^{-4}	3.93	9.08×10^{-7}	7.45	1.04×10^{-8}	11.95
0.1	8.15×10^{-6}	3.99	9.29×10^{-9}	6.61	1.05×10^{-10}	6.63
δt	Radau 5		Radau 7		Radau 9	
	Error	Rate	Error	Rate	Error	Rate
0.4	2.37×10^{-4}	—	3.96×10^{-6}	—	6.21×10^{-8}	—
0.2	8.35×10^{-6}	4.83	3.54×10^{-8}	6.81	1.42×10^{-10}	8.77
0.1	2.71×10^{-7}	4.94	2.93×10^{-10}	6.91	3.64×10^{-11}	1.96
δt	Lobatto 4		Lobatto 6		Lobatto 8	
	Error	Rate	Error	Rate	Error	Rate
0.4	2.42×10^{-3}	—	3.93×10^{-5}	—	6.15×10^{-7}	—
0.2	1.78×10^{-4}	3.76	7.23×10^{-7}	5.77	2.86×10^{-9}	7.75
0.1	1.18×10^{-5}	3.92	1.19×10^{-8}	5.91	3.62×10^{-11}	6.30

Euler time integration. The new methods are shown to achieve fast, high-order accuracy on multiple different compressible and incompressible Navier Stokes and Euler problems. Using low-order Gauss integration schemes with the new method consistently requires about half the preconditioner applications as required by standard SDIRK schemes to achieve the same accuracy, demonstrating that the new method can not only offer very high-order accuracy (along with other benefits obtained by using fully implicit Runge-Kutta), but also improve upon state-of-the-art low-order integration. Moreover, for the incompressible Navier Stokes double shear layer problem in vorticity-streamfunction form, one can apply 7th to 10th order Gauss or Radau IIA integration for a comparable number of preconditioner applications as standard 4th-order SDIRK.

A Proof

Proof of Theorem 2. As in [46, Th. 5], the square of the condition number of \mathcal{P}_γ is given by

$$\kappa^2(\mathcal{P}_\gamma) = \|\mathcal{P}_\gamma\|^2 \|\mathcal{P}_\gamma^{-1}\|^2 = \max_{\mathbf{v} \neq 0} \frac{\|\mathcal{P}_\gamma \mathbf{v}\|^2}{\|\mathbf{v}\|^2} \frac{1}{\min_{\mathbf{v} \neq 0} \frac{\|\mathcal{P}_\gamma \mathbf{v}\|^2}{\|\mathbf{v}\|^2}}. \quad (43)$$

First, consider bounding $\|\mathcal{P}_\gamma\|$ for $\gamma \geq \eta$. Expanding (19) yields an equivalent form

$$\begin{aligned} \mathcal{P}_\gamma &= \left[\eta I - \widehat{\mathcal{L}}_2 + \beta^2 (\eta I - \widehat{\mathcal{L}}_1)^{-1} \right] (\gamma I - \widehat{\mathcal{L}}_2)^{-1} \\ &= I - (\gamma - \eta) (\gamma I - \widehat{\mathcal{L}}_2)^{-1} + \beta^2 (\eta I - \widehat{\mathcal{L}}_1)^{-1} (\gamma I - \widehat{\mathcal{L}}_2)^{-1}. \end{aligned}$$

Then,

$$\begin{aligned} \|\mathcal{P}_\gamma\| &\leq \left\| I - (\gamma - \eta) (\gamma I - \widehat{\mathcal{L}}_2)^{-1} \right\| + \frac{\beta^2}{\gamma \eta} \left\| (I - \frac{1}{\eta} \widehat{\mathcal{L}}_1)^{-1} \right\| \left\| (I - \frac{1}{\gamma} \widehat{\mathcal{L}}_2)^{-1} \right\| \\ &\leq \left\| I - (\gamma - \eta) (\gamma I - \widehat{\mathcal{L}}_2)^{-1} \right\| + \frac{\beta^2}{\gamma \eta}. \end{aligned} \quad (44)$$

The last inequality follows by noting

$$\begin{aligned} \sup_{\mathbf{v} \neq \mathbf{0}} \frac{\|(I - \frac{1}{\gamma} \widehat{\mathcal{L}}_2)^{-1} \mathbf{v}\|^2}{\|\mathbf{v}\|^2} &= \sup_{\mathbf{w} \neq \mathbf{0}} \frac{\|\mathbf{w}\|^2}{\|(I - \frac{1}{\gamma} \widehat{\mathcal{L}}_2) \mathbf{w}\|^2} \\ &= \sup_{\mathbf{w} \neq \mathbf{0}} \frac{\|\mathbf{w}\|^2}{\|\mathbf{w}\|^2 - \frac{2}{\gamma} \langle \widehat{\mathcal{L}}_2 \mathbf{w}, \mathbf{w} \rangle + \frac{1}{\gamma^2} \|\widehat{\mathcal{L}}_2 \mathbf{w}\|^2} \leq 1, \end{aligned}$$

because all terms in the denominator are nonnegative. For the first term in (44), note that maximizing over $\mathbf{v} \in \mathbb{R}^n$ and letting $\mathbf{v} \mapsto (\gamma I - \widehat{\mathcal{L}}_2) \mathbf{w}$,

$$\begin{aligned} \left\| I - (\gamma - \eta)(\gamma I - \widehat{\mathcal{L}}_2)^{-1} \right\|^2 &= \sup_{\mathbf{w} \neq \mathbf{0}} \frac{\|(\gamma I - \widehat{\mathcal{L}}_2 - (\gamma - \eta)I) \mathbf{w}\|^2}{\|(\gamma I - \widehat{\mathcal{L}}_2) \mathbf{w}\|^2} \\ &= \sup_{\mathbf{w} \neq \mathbf{0}} \frac{\eta^2 \|\mathbf{w}\|^2 - 2\eta \langle \widehat{\mathcal{L}}_2 \mathbf{w}, \mathbf{w} \rangle + \|\widehat{\mathcal{L}}_2 \mathbf{w}\|^2}{\gamma^2 \|\mathbf{w}\|^2 - 2\gamma \langle \widehat{\mathcal{L}}_2 \mathbf{w}, \mathbf{w} \rangle + \|\widehat{\mathcal{L}}_2 \mathbf{w}\|^2}. \end{aligned}$$

By Assumptions 1 and 2, $W(\widehat{\mathcal{L}}_2) \leq 0$ and $\eta > 0$, implying all terms in the numerator and denominator are nonnegative. Moreover, by assumption $\gamma \geq \eta$, implying all numerator terms are bounded above by the matching denominator terms, which yields $\|I - (\gamma - \eta)(\gamma I - \widehat{\mathcal{L}}_2)^{-1}\| \leq 1$. Combining with (44) yields

$$\|\mathcal{P}_\gamma\| \leq 1 + \frac{\beta^2}{\gamma\eta}. \quad (45)$$

Now consider bounding $\|\mathcal{P}_\gamma^{-1}\|$ from above. Consistent with (43), we do so by considering the minimum singular value, $\|\mathcal{P}_\gamma^{-1}\| = \frac{1}{s_{\min}(\mathcal{P}_\gamma)}$, where $s_{\min}(\mathcal{P}_\gamma) = \min_{\mathbf{v} \neq \mathbf{0}} \frac{\|\mathcal{P}_\gamma \mathbf{v}\|}{\|\mathbf{v}\|}$. Letting $\mathbf{v} \mapsto (\gamma I - \widehat{\mathcal{L}}_2)(\eta I - \widehat{\mathcal{L}}_1) \mathbf{w}$ in the ratio $\|\mathcal{P}_\gamma \mathbf{v}\|/\|\mathbf{v}\|$, and expanding the numerator (see inner term in (19)) yields

$$\begin{aligned} s_{\min}(\mathcal{P}_\gamma)^2 &= \min_{\mathbf{w} \neq \mathbf{0}} \frac{\left\| \left[(\eta^2 + \beta^2)I - \eta(\widehat{\mathcal{L}}_1 + \widehat{\mathcal{L}}_2) + \widehat{\mathcal{L}}_2 \widehat{\mathcal{L}}_1 \right] \mathbf{w} \right\|^2}{\|(\gamma I - \widehat{\mathcal{L}}_2)(\eta I - \widehat{\mathcal{L}}_1) \mathbf{w}\|^2} \\ &= \min_{\mathbf{w} \neq \mathbf{0}} \frac{\left\| \left[(\gamma I - \widehat{\mathcal{L}}_2)(\eta I - \widehat{\mathcal{L}}_1) + (\gamma - \eta)\widehat{\mathcal{L}}_1 + (\eta^2 + \beta^2 - \gamma\eta)I \right] \mathbf{w} \right\|^2}{\|(\gamma I - \widehat{\mathcal{L}}_2)(\eta I - \widehat{\mathcal{L}}_1) \mathbf{w}\|^2}. \end{aligned}$$

Here, we make the strategic choice of γ such that the identity perturbation $(\eta^2 + \beta^2 - \gamma\eta)I = \mathbf{0}$, given by $\gamma_* := \frac{\eta^2 + \beta^2}{\eta}$ (23). Expanding,

$$\begin{aligned} s_{\min}(\mathcal{P}_{\gamma_*})^2 &= \min_{\mathbf{w} \neq \mathbf{0}} \frac{\left\| \left[(\gamma_* I - \widehat{\mathcal{L}}_2)(\eta I - \widehat{\mathcal{L}}_1) + \frac{\beta^2}{\eta} \widehat{\mathcal{L}}_1 \right] \mathbf{w} \right\|^2}{\|(\gamma_* I - \widehat{\mathcal{L}}_2)(\eta I - \widehat{\mathcal{L}}_1) \mathbf{w}\|^2} \\ &= \min_{\mathbf{w} \neq \mathbf{0}} 1 + \frac{\beta^2}{\eta} \cdot \frac{\frac{\beta^2}{\eta} \|\widehat{\mathcal{L}}_1 \mathbf{w}\|^2 + 2 \langle (\gamma_* I - \widehat{\mathcal{L}}_2)(\eta I - \widehat{\mathcal{L}}_1) \mathbf{w}, \widehat{\mathcal{L}}_1 \mathbf{w} \rangle}{\|(\gamma_* I - \widehat{\mathcal{L}}_2)(\eta I - \widehat{\mathcal{L}}_1) \mathbf{w}\|^2} \\ &= 1 - \frac{\beta^2}{\eta} \cdot \max_{\mathbf{w} \neq \mathbf{0}} \frac{-2 \langle (\gamma_* I - \widehat{\mathcal{L}}_2)(\eta I - \widehat{\mathcal{L}}_1) \mathbf{w}, \widehat{\mathcal{L}}_1 \mathbf{w} \rangle - \frac{\beta^2}{\eta} \|\widehat{\mathcal{L}}_1 \mathbf{w}\|^2}{\|(\gamma_* I - \widehat{\mathcal{L}}_2)(\eta I - \widehat{\mathcal{L}}_1) \mathbf{w}\|^2}. \end{aligned} \quad (46)$$

Expanding the numerator in (46) yields

$$-2 \langle (\gamma_* I - \widehat{\mathcal{L}}_2)(\eta I - \widehat{\mathcal{L}}_1) \mathbf{w}, \widehat{\mathcal{L}}_1 \mathbf{w} \rangle - \frac{\beta^2}{\eta} \|\widehat{\mathcal{L}}_1 \mathbf{w}\|^2$$

$$\begin{aligned}
&= \left(2\gamma_* - \frac{\beta^2}{\eta}\right) \|\widehat{\mathcal{L}}_1 \mathbf{w}\|^2 - 2\gamma_* \eta \langle \widehat{\mathcal{L}}_1 \mathbf{w}, \mathbf{w} \rangle - 2\langle \widehat{\mathcal{L}}_2(\widehat{\mathcal{L}}_1 \mathbf{w}), \widehat{\mathcal{L}}_1 \mathbf{w} \rangle + 2\eta \langle \widehat{\mathcal{L}}_1 \mathbf{w}, \widehat{\mathcal{L}}_2 \mathbf{w} \rangle \\
&= \frac{2\eta^2 + \beta^2}{\eta} \|\widehat{\mathcal{L}}_1 \mathbf{w}\|^2 - 2(\eta^2 + \beta^2) \langle \widehat{\mathcal{L}}_1 \mathbf{w}, \mathbf{w} \rangle - 2\langle \widehat{\mathcal{L}}_2(\widehat{\mathcal{L}}_1 \mathbf{w}), \widehat{\mathcal{L}}_1 \mathbf{w} \rangle + 2\eta \langle \widehat{\mathcal{L}}_1 \mathbf{w}, \widehat{\mathcal{L}}_2 \mathbf{w} \rangle. \tag{47}
\end{aligned}$$

Now consider the denominator:

$$\begin{aligned}
&\|(\gamma_* I - \widehat{\mathcal{L}}_2)(\eta I - \widehat{\mathcal{L}}_1) \mathbf{w}\|^2 = \|(\gamma_* \eta I + \widehat{\mathcal{L}}_2 \widehat{\mathcal{L}}_1) \mathbf{w} - (\eta \widehat{\mathcal{L}}_2 + \gamma_* \widehat{\mathcal{L}}_1) \mathbf{w}\|^2 \\
&= \|(\gamma_* \eta I + \widehat{\mathcal{L}}_2 \widehat{\mathcal{L}}_1) \mathbf{w}\|^2 + \eta^2 \|\widehat{\mathcal{L}}_2 \mathbf{w}\|^2 + \gamma_*^2 \|\widehat{\mathcal{L}}_1 \mathbf{w}\|^2 + 2\gamma_* \eta \langle \widehat{\mathcal{L}}_1 \mathbf{w}, \widehat{\mathcal{L}}_2 \mathbf{w} \rangle \\
&\quad - 2\eta \langle (\gamma_* \eta I + \widehat{\mathcal{L}}_2 \widehat{\mathcal{L}}_1) \mathbf{w}, \widehat{\mathcal{L}}_2 \mathbf{w} \rangle - 2\gamma_* \langle (\gamma_* \eta I + \widehat{\mathcal{L}}_2 \widehat{\mathcal{L}}_1) \mathbf{w}, \widehat{\mathcal{L}}_1 \mathbf{w} \rangle \\
&\geq \|(\gamma_* \eta I + \widehat{\mathcal{L}}_2 \widehat{\mathcal{L}}_1) \mathbf{w}\|^2 + \eta^2 \|\widehat{\mathcal{L}}_2 \mathbf{w}\|^2 + \gamma_*^2 \|\widehat{\mathcal{L}}_1 \mathbf{w}\|^2 + 2\gamma_* \eta \langle \widehat{\mathcal{L}}_1 \mathbf{w}, \widehat{\mathcal{L}}_2 \mathbf{w} \rangle \\
&\quad - 2\eta \left\| (\gamma_* \eta I + \widehat{\mathcal{L}}_2 \widehat{\mathcal{L}}_1) \mathbf{w} \right\| \|\widehat{\mathcal{L}}_2 \mathbf{w}\| - 2\gamma_* \langle (\gamma_* \eta I + \widehat{\mathcal{L}}_2 \widehat{\mathcal{L}}_1) \mathbf{w}, \widehat{\mathcal{L}}_1 \mathbf{w} \rangle \\
&= \left(\left\| (\gamma_* \eta I + \widehat{\mathcal{L}}_2 \widehat{\mathcal{L}}_1) \mathbf{w} \right\| - \eta \|\widehat{\mathcal{L}}_2 \mathbf{w}\| \right)^2 + \gamma_*^2 \|\widehat{\mathcal{L}}_1 \mathbf{w}\|^2 \\
&\quad - 2\gamma_* \langle (\gamma_* \eta I + \widehat{\mathcal{L}}_2 \widehat{\mathcal{L}}_1) \mathbf{w}, \widehat{\mathcal{L}}_1 \mathbf{w} \rangle + 2\gamma_* \eta \langle \widehat{\mathcal{L}}_1 \mathbf{w}, \widehat{\mathcal{L}}_2 \mathbf{w} \rangle \\
&\geq \gamma_*^2 \|\widehat{\mathcal{L}}_1 \mathbf{w}\|^2 - 2\gamma_*^2 \eta \langle \widehat{\mathcal{L}}_1 \mathbf{w}, \mathbf{w} \rangle - 2\gamma_* \langle \widehat{\mathcal{L}}_2(\widehat{\mathcal{L}}_1 \mathbf{w}), \widehat{\mathcal{L}}_1 \mathbf{w} \rangle + 2\gamma_* \eta \langle \widehat{\mathcal{L}}_1 \mathbf{w}, \widehat{\mathcal{L}}_2 \mathbf{w} \rangle. \tag{48}
\end{aligned}$$

Notice that we now have matching terms in expressions for the numerator (47) and denominator (48). Moreover, by assumption $\langle \widehat{\mathcal{L}}_1 \mathbf{w}, \widehat{\mathcal{L}}_2 \mathbf{w} \rangle \geq 0$, and thus all terms in (47) and (48) are non-negative. Returning to the minimum singular value defined in (46) and plugging in the numerator (47) and denominator bounds (48), we can bound the total ratio by considering the maximum ratio between matching numerator and denominator terms:

$$\begin{aligned}
&\max_{\mathbf{w} \neq \mathbf{0}} \frac{-2 \langle (\gamma_* I - \widehat{\mathcal{L}}_2)(\eta I - \widehat{\mathcal{L}}_1) \mathbf{w}, \widehat{\mathcal{L}}_1 \mathbf{w} \rangle - \frac{\beta^2}{\eta} \|\widehat{\mathcal{L}}_1 \mathbf{w}\|^2}{\|(\gamma_* I - \widehat{\mathcal{L}}_2)(\eta I - \widehat{\mathcal{L}}_1) \mathbf{w}\|^2} \\
&\leq \max_{\mathbf{w} \neq \mathbf{0}} \frac{\frac{2\eta^2 + \beta^2}{\eta} \|\widehat{\mathcal{L}}_1 \mathbf{w}\|^2 - 2(\eta^2 + \beta^2) \langle \widehat{\mathcal{L}}_1 \mathbf{w}, \mathbf{w} \rangle - 2\langle \widehat{\mathcal{L}}_2(\widehat{\mathcal{L}}_1 \mathbf{w}), \widehat{\mathcal{L}}_1 \mathbf{w} \rangle + 2\eta \langle \widehat{\mathcal{L}}_1 \mathbf{w}, \widehat{\mathcal{L}}_2 \mathbf{w} \rangle}{\gamma_*^2 \|\widehat{\mathcal{L}}_1 \mathbf{w}\|^2 - 2\gamma_*^2 \eta \langle \widehat{\mathcal{L}}_1 \mathbf{w}, \mathbf{w} \rangle - 2\gamma_* \langle \widehat{\mathcal{L}}_2(\widehat{\mathcal{L}}_1 \mathbf{w}), \widehat{\mathcal{L}}_1 \mathbf{w} \rangle + 2\gamma_* \eta \langle \widehat{\mathcal{L}}_1 \mathbf{w}, \widehat{\mathcal{L}}_2 \mathbf{w} \rangle} \\
&\leq \max \left\{ \frac{\eta(2\eta^2 + \beta^2)}{(\eta^2 + \beta^2)^2}, \frac{\eta}{\eta^2 + \beta^2}, \frac{\eta}{\eta^2 + \beta^2}, \frac{\eta}{\eta^2 + \beta^2} \right\} \\
&= \frac{\eta(2\eta^2 + \beta^2)}{(\eta^2 + \beta^2)^2}. \tag{49}
\end{aligned}$$

Simplifying and plugging in to (46) yields

$$s_{\min}(\mathcal{P}_{\gamma_*})^2 \geq 1 - \frac{\beta^2}{\eta} \cdot \frac{\eta(2\eta^2 + \beta^2)}{(\eta^2 + \beta^2)^2} = \frac{\eta^4}{(\eta^2 + \beta^2)^2}. \tag{50}$$

Applying $\|\mathcal{P}_\gamma^{-1}\| = \frac{1}{s_{\min}(\mathcal{P}_\gamma)}$, to (50) and combining with (45) yields

$$\kappa(\mathcal{P}_{\gamma_*}) = \|\mathcal{P}_{\gamma_*}\| \|\mathcal{P}_{\gamma_*}^{-1}\| \leq \left(1 + \frac{\eta^2}{\eta^2 + \beta^2}\right) \frac{\eta^2 + \beta^2}{\eta^2} = 2 + \frac{\beta^2}{\eta^2}. \tag{51}$$

□

Acknowledgments

This work was performed under the auspices of the U.S. Department of Energy by Lawrence Livermore National Laboratory under Contract DE-AC52-07NA27344 (LLNL-JRNL-817953).

Los Alamos National Laboratory report number LA-UR-20-30412. This document was prepared as an account of work sponsored by an agency of the United States government. Neither the United States government nor Lawrence Livermore National Security, LLC, nor any of their employees makes any warranty, expressed or implied, or assumes any legal liability or responsibility for the accuracy, completeness, or usefulness of any information, apparatus, product, or process disclosed, or represents that its use would not infringe privately owned rights. Reference herein to any specific commercial product, process, or service by trade name, trademark, manufacturer, or otherwise does not necessarily constitute or imply its endorsement, recommendation, or favoring by the United States government or Lawrence Livermore National Security, LLC. The views and opinions of authors expressed herein do not necessarily state or reflect those of the United States government or Lawrence Livermore National Security, LLC, and shall not be used for advertising or product endorsement purposes.

References

- [1] G. AKRIVIS, C. MAKRIDAKIS, AND R. H. NOCHETTO, *Galerkin and Runge-Kutta methods: unified formulation, a posteriori error estimates and nodal superconvergence*, Numerische Mathematik, 118 (2011), pp. 429–456.
- [2] R. ANDERSON, J. ANDREJ, A. BARKER, J. BRAMWELL, J.-S. CAMIER, J. CERVENY, V. DOBREV, Y. DUDOUIT, A. FISHER, T. KOLEV, W. PAZNER, M. STOWELL, V. TOMOV, J. DAHM, D. MEDINA, AND S. ZAMPINI, *MFEM: a modular finite element methods library*, Computers & Mathematics with Applications, (2020).
- [3] D. N. ARNOLD, *An interior penalty finite element method with discontinuous elements*, SIAM Journal on Numerical Analysis, 19 (1982), pp. 742–760.
- [4] S. BASTING AND E. BÄNSCH, *Preconditioners for the Discontinuous Galerkin time-stepping method of arbitrary order*, ESAIM: Mathematical Modelling and Numerical Analysis, 51 (2017), pp. 1173–1195.
- [5] J. B. BELL, P. COLELLA, AND H. M. GLAZ, *A second-order projection method for the incompressible Navier–Stokes equations*, Journal of Computational Physics, 85 (1989), pp. 257–283.
- [6] T. A. BICKART, *An Efficient Solution Process for Implicit Runge–Kutta Methods*, SIAM Journal on Numerical Analysis, 14 (1977), pp. 1022–1027.
- [7] K. E. BRENNAN, S. L. CAMPBELL, AND L. R. PETZOLD, *Numerical solution of initial-value problems in differential-algebraic equations*, SIAM, 1995.
- [8] J. C. BUTCHER, *On the implementation of implicit Runge-Kutta methods*, BIT Numerical Mathematics, 16 (1976), pp. 237–240.
- [9] H. CHEN, *A splitting preconditioner for the iterative solution of implicit Runge-Kutta and boundary value methods*, BIT Numerical Mathematics, 54 (2014), pp. 607–621.
- [10] G. J. COOPER AND J. C. BUTCHER, *An iteration scheme for implicit Runge-Kutta methods*, IMA Journal of Numerical Analysis, 3 (1983), pp. 127–140.
- [11] G. J. COOPER AND R. VIGNESVARAN, *A scheme for the implementation of implicit Runge-Kutta methods*, Computing, 45 (1990), pp. 321–332.

- [12] P. E. FARRELL, R. C. KIRBY, AND J. MARCHENA-MENENDEZ, *Irksome: Automating runge-kutta time-stepping for finite element methods*, arXiv preprint arXiv:2006.16282, (2020).
- [13] S. GONZÁLEZ-PINTO, J. MONTIJANO, AND L. RÁNDEZ, *Iterative schemes for three-stage implicit Runge-Kutta methods*, Applied Numerical Mathematics, 17 (1995), pp. 363–382.
- [14] S. GONZÁLEZ-PINTO, J. MONTIJANO, AND L. RÁNDEZ, *Improving the efficiency of the iterative schemes for implicit Runge-Kutta methods*, Journal of Computational and Applied Mathematics, 66 (1996), pp. 227–238.
- [15] E. HAIRER AND G. WANNER, *Solving Ordinary Differential Equations II, Stiff and Differential-Algebraic Problems*, (1996), pp. 118–130.
- [16] E. HAIRER AND G. WANNER, *Stiff differential equations solved by Radau methods*, Journal of Computational and Applied Mathematics, 111 (1999), pp. 93–111.
- [17] E. HAIRER, G. WANNER, AND C. LUBICH, *Geometric Numerical Integration, Structure-Preserving Algorithms for Ordinary Differential Equations*, (2002).
- [18] W. HOFFMANN AND J. J. B. D. SWART, *Approximating Runge-Kutta matrices by triangular matrices*, BIT Numerical Mathematics, 37 (1997), pp. 346–354.
- [19] P. J. V. D. HOUWEN AND J. J. B. D. SWART, *Parallel linear system solvers for Runge-Kutta methods*, Advances in Computational Mathematics, 7 (1997), pp. 157–181.
- [20] L. O. JAY, *Inexact Simplified Newton Iterations for Implicit Runge-Kutta Methods*, SIAM Journal on Numerical Analysis, 38 (2000), pp. 1369–1388.
- [21] L. O. JAY AND T. BRACONNIER, *A parallelizable preconditioner for the iterative solution of implicit Runge-Kutta-type methods*, Journal of Computational and Applied Mathematics, 111 (1999), pp. 63–76.
- [22] X. JIAO, X. WANG, AND Q. CHEN, *Optimal and low-memory near-optimal preconditioning of fully implicit runge-kutta schemes for parabolic pdes*, arXiv preprint arXiv:2012.12779, (2020).
- [23] S. KANNER AND P.-O. PERSSON, *Validation of a high-order large-eddy simulation solver using a vertical-axis wind turbine*, AIAA Journal, 54 (2015), pp. 101–112.
- [24] C. KENNEDY AND M. H. CARPENTER, *Diagonally Implicit Runge-Kutta Methods for Ordinary Differential Equations. A Review*, tech. report, 2016.
- [25] P. LASAINT AND P. RAVIART, *On a finite element method for solving the neutron transport equation*, Mathematical Aspects of Finite Elements in Partial Differential Equations, (1974), pp. 89–123.
- [26] J. V. LENT AND S. VANDEWALLE, *Multigrid Methods for Implicit Runge-Kutta and Boundary Value Method Discretizations of Parabolic PDEs*, SIAM Journal on Scientific Computing, 27 (2005), pp. 67–92.
- [27] R. J. LEVEQUE, *Finite Difference Methods for Ordinary and Partial Differential Equations: Steady-State and Time-Dependent Problems*, vol. 98, Siam, 2007.
- [28] J.-G. LIU AND C.-W. SHU, *A high-order discontinuous Galerkin method for 2D incompressible flows*, Journal of Computational Physics, 160 (2000), pp. 577–596.

- [29] C. MAKRIDAKIS AND R. H. NOCHETTO, *A posteriori error analysis for higher order dissipative methods for evolution problems*, Numerische Mathematik, 104 (2006), pp. 489–514.
- [30] T. A. MANTEUFFEL, S. MÜNZENMAIER, J. RUGE, AND B. S. SOUTHWORTH, *Non-symmetric reduction-based algebraic multigrid*, SIAM J. Sci. Comput., 41 (2019), pp. S242–S268.
- [31] T. A. MANTEUFFEL, J. RUGE, AND B. S. SOUTHWORTH, *Nonsymmetric algebraic multigrid based on local approximate ideal restriction (ℓ AIR)*, SIAM J. Sci. Comput., 40 (2018), pp. A4105–A4130.
- [32] K. A. MARDAL, T. K. NILSSEN, AND G. A. STAFF, *Order-Optimal Preconditioners for Implicit Runge–Kutta Schemes Applied to Parabolic PDEs*, SIAM Journal on Scientific Computing, 29 (2007), pp. 361–375.
- [33] T. K. NILSSEN, G. A. STAFF, AND K. MARDAL, *Order optimal preconditioners for fully implicit Runge-Kutta schemes applied to the bidomain equations*, Numerical Methods for Partial Differential Equations, 27 (2011), pp. 1290–1312.
- [34] W. PAZNER AND P.-O. PERSSON, *Stage-parallel fully implicit Runge–Kutta solvers for discontinuous Galerkin fluid simulations*, Journal of Computational Physics, 335 (2017), pp. 700–717.
- [35] J. PERAIRE AND P.-O. PERSSON, *The compact discontinuous Galerkin (CDG) method for elliptic problems*, SIAM Journal on Scientific Computing, 30 (2008), pp. 1806–1824.
- [36] P.-O. PERSSON AND J. PERAIRE, *Newton-GMRES preconditioning for discontinuous Galerkin discretizations of the Navier–Stokes equations*, SIAM Journal on Scientific Computing, 30 (2008), pp. 2709–2733.
- [37] M. M. RANA, V. E. HOWLE, K. LONG, A. MEEK, AND W. MILESTONE, *A new block preconditioner for implicit runge-kutta methods for parabolic pde*, arXiv preprint arXiv:2010.11377, (2020).
- [38] S. C. REDDY AND L. N. TREFETHEN, *Stability of the method of lines*, Numerische Mathematik, 62 (1992), pp. 235–267.
- [39] T. RICHTER, A. SPRINGER, AND B. VEXLER, *Efficient numerical realization of discontinuous Galerkin methods for temporal discretization of parabolic problems*, Numerische Mathematik, 124 (2013), pp. 151–182.
- [40] P. L. ROE, *Approximate Riemann solvers, parameter vectors, and difference schemes*, Journal of Computational Physics, 43 (1981), pp. 357–372.
- [41] R. R. ROSALES, B. SEIBOLD, D. SHIROKOFF, AND D. ZHOU, *Spatial manifestations of order reduction in runge-kutta methods for initial boundary value problems*, arXiv preprint arXiv:1712.00897, (2017).
- [42] B. SANDERSE, *Energy-conserving Runge–Kutta methods for the incompressible Navier–Stokes equations*, Journal of Computational Physics, 233 (2013), pp. 100–131.
- [43] D. SCHÖTZAU AND C. SCHWAB, *Time Discretization of Parabolic Problems by the HP-Version of the Discontinuous Galerkin Finite Element Method*, SIAM Journal on Numerical Analysis, 38 (2000), pp. 837–875.

- [44] C.-W. SHU, *Essentially non-oscillatory and weighted essentially non-oscillatory schemes for hyperbolic conservation laws*, in *Lecture Notes in Mathematics*, Springer Berlin Heidelberg, 1998, pp. 325–432.
- [45] I. SMEARS, *Robust and efficient preconditioners for the discontinuous Galerkin time-stepping method*, *IMA Journal of Numerical Analysis*, (2016), p. drw050.
- [46] B. S. SOUTHWORTH, O. A. KRZYSIK, W. PAZNER, AND H. DE STERCK, *Fast solution of fully implicit Runge-Kutta and discontinuous Galerkin in time for numerical PDEs, part I: the linear setting*, arXiv preprint arXiv:2101.00512, (2021).
- [47] B. S. SOUTHWORTH, A. A. SIVAS, AND S. RHEBERGEN, *On fixed-point, Krylov, and 2x2 block preconditioners for nonsymmetric problems*, *SIAM Journal on Matrix Analysis and Applications*, 41 (2020), pp. 871–900.
- [48] G. A. STAFF, K.-A. MARDAL, AND T. K. NILSSEN, *Preconditioning of fully implicit Runge-Kutta schemes for parabolic PDEs*, *Modeling, Identification and Control: A Norwegian Research Bulletin*, 27 (2006), pp. 109–123.
- [49] L. N. TREFETHEN AND M. EMBREE, *Spectra and pseudospectra: the behavior of nonnormal matrices and operators*, Princeton University Press, 2005.
- [50] J. M. VARAH, *On the efficient implementation of implicit Runge-Kutta methods*, *Mathematics of Computation*, 33 (1979), pp. 557–557.
- [51] Z. WANG, K. FIDKOWSKI, R. ABGRALL, F. BASSI, D. CARAENI, A. CARY, H. DECONINCK, R. HARTMANN, K. HILLEWAERT, H. HUYNH, AND ET AL., *High-order CFD methods: current status and perspective*, *International Journal for Numerical Methods in Fluids*, 72 (2013), pp. 811–845.